

# Flavour specific neutrino self-interaction: $H_0$ tension and IceCube

Arindam Mazumdar,<sup>a</sup> Subhendra Mohanty,<sup>b</sup> Priyank Parashari<sup>b,c</sup>

<sup>a</sup>Centre for Theoretical Studies, Indian Institute of Technology, Kharagpur 721302, India

<sup>b</sup>Physical Research Laboratory, Ahmedabad, 380009, India

<sup>c</sup>Centre for High Energy Physics, Indian Institute of Science, C. V. Raman Avenue, Bengaluru 560012, India

E-mail: [arindam.mazumdar@iitkgp.ac.in](mailto:arindam.mazumdar@iitkgp.ac.in), [mohanty@prl.res.in](mailto:mohanty@prl.res.in), [ppriyank@iisc.ac.in](mailto:ppriyank@iisc.ac.in)

**Abstract.** Self-interaction in the active neutrinos is studied in the literature to alleviate the  $H_0$  tension. Similar self-interaction can also explain the observed dips in the flux of the neutrinos coming from the distant astro-physical sources in IceCube detectors. In contrast to the flavour universal neutrino interaction considered for solving the  $H_0$  tension, which is ruled out from particle physics experiments, we consider flavour specific neutrino interactions. We show that the values of self-interaction coupling constant and mediator mass required for explaining the IceCube dips are inconsistent with the strong neutrino self-interactions preferred by the combination of BAO, HST and Planck data. However, the required amount of self-interaction between tau neutrinos ( $\nu_\tau$ ) in inverted hierarchy for explaining IceCube dips is consistent with the moderate self-interaction region of cosmological bounds at 1- $\sigma$  level. For the case of other interactions and hierarchies, the IceCube preferred amount of self-interaction is consistent with moderate self-interaction region of cosmological bounds at 2- $\sigma$  level only.

**Keywords:** Massive neutrinos, Self interaction,  $H_0$  Tension, IceCube, CMB,

---

## Contents

<b>1</b>	<b>Introduction</b>	<b>1</b>
<b>2</b>	<b>Self-interaction in neutrinos</b>	<b>3</b>
<b>3</b>	<b>Constraints from cosmological data set</b>	<b>5</b>
<b>4</b>	<b>Neutrino absorption by Cosmic Neutrino Background</b>	<b>9</b>
<b>5</b>	<b>Parameter estimation from flux at IceCube</b>	<b>12</b>
5.1	Normal hierarchy	13
5.2	Inverted Hierarchy	15
<b>6</b>	<b>Conclusions</b>	<b>18</b>
<b>A</b>	<b>Numerical details</b>	<b>20</b>

---

## 1 Introduction

Self-interaction in between the neutrinos has been an active topic of interest in different sectors of cosmology [1–8], astro-physics [9, 10] and laboratory based neutrino experiments [11–13]. In the recent years it has been studied extensively in the context of  $H_0$  tension [3, 4]. Moreover, if this self-interaction is mediated by some MeV scale boson then the resonant on-shell production of mediator in the collision between the astro-physical neutrinos and the cosmic neutrino background can create some signature in the observed IceCube PeV neutrino flux [14–17]. In this paper we check if these two types of applications of self-interaction in neutrinos are consistent with each other or not.

There is a discrepancy between the determination of the Hubble constant  $H_0$  from Planck [18] (which assumes the  $\Lambda$ CDM cosmology) and those from local measurements based on distance ladder and time delay in lensing observations which points to new physics beyond the  $\Lambda$ CDM model [19–22]. The Planck observation finds the value  $H_0 = (67.27 \pm 0.60)$  km/s/Mpc which is in  $4.4\sigma$  disagreement compared for example to the SHOES collaboration [23] determination of  $H_0 = (74.03 \pm 1.42)$  km/s/Mpc, based on the observations by the Hubble Space Telescope of Cepheids in the Large Magellanic Cloud. One of the ways to alleviate the  $H_0$  tension is to have a large self-interaction between neutrinos [3]. Self-interaction delays the free-streaming of neutrinos and neutrinos cluster at smaller length scales. This is compensated by increasing  $H_0$ . In ref. [3] the best fit value of  $H_0$  which is closer to the distance ladder values was obtained by taking an effective neutrino self-interaction  $\mathcal{L} = G_{\text{eff}}(\bar{\nu}\nu)(\bar{\nu}\nu)$  with  $G_{\text{eff}}$  having two preferred values where moderate self-interaction (MI) has  $\log_{10}(G_{\text{eff}}\text{MeV}^2) = -3.90^{+1.0}_{-0.93}$  and strong self-interaction (SI) has  $\log_{10}(G_{\text{eff}}\text{MeV}^2) = -1.35^{+0.12}_{-0.066}$ . In a similar analysis in ref. [4], it is shown that when considering only WMAP data, which measures TT anisotropy spectrum up to multipole  $l \leq 1200$ , the bimodal peaks in the probability of  $\log_{10}(G_{\text{eff}}\text{MeV}^2)$  disappears and neutrino self interactions are consistent with zero. The bimodal distribution of  $\log_{10}(G_{\text{eff}}\text{MeV}^2)$  appears when Planck TT and TE data between  $1200 \leq l \leq 2500$  are included.

In ref. [3] and [4] (and in earlier studies of CMB with neutrino self-interactions [2], [1]) the neutrino self-interaction that is considered is identical for all neutrino flavours. It has been pointed out that such large flavour universal couplings of neutrinos which implies mediator masses of  $\mathcal{O}(\text{MeV})$  is severely constrained from particle physics. Strong bounds on  $\nu$  self-interactions come from meson decays [12, 24], neutrino-less double beta decay [25] and from  $Z$  and  $\tau$  decays [13]. Neutrino-less double beta decays rule out Majoron mediated  $\nu_e$  interactions as a solution to the  $H_0$  tension [25]. Decays of  $\pi^+/K^+$  to  $e^+\nu_e$  and  $\mu^+\nu_\mu$  put strong constraints on  $\nu_e$  and  $\nu_\mu$  interactions while the constraints on  $\nu_\tau$  couplings are determined only from  $D_s^+ \rightarrow \tau^+\nu_\tau$  which is not so well constrained [12, 24]. The  $Z$  and  $\tau$  invisible decay width give the strongest bounds for heavy scalar mediators ( $m_\phi > 300\text{MeV}$ ) couplings to  $\nu_\tau$  [13]. To summarize, particle physics allows the self-interactions of  $\nu_\tau$  in the MI region ( $m_\phi \sim 10 - 100\text{MeV}$ ) while universal flavour coupling interaction explored by refs. [3, 4] in context of  $H_0$  tension is ruled out as shown in ref. [12].

In this paper, we consider flavour specific self-interactions between neutrinos and study their effect on CMB power spectrum. We consider four cases :  $\nu_e, \nu_\mu, \nu_\tau$  and the flavour universal self-interactions. From the CMB analysis we find that there is no discernible difference between the  $\nu_\tau$  self-interactions allowed from particle physics constraints and the universal flavour interactions. We find, similar to the earlier papers [1–4], that  $\log_{10}(G_{\text{eff}}\text{MeV}^2)$  has a bimodal distribution in probability with a SI and MI peak. The allowed values of  $N_{\text{eff}}$  for the joint analysis of Planck CMB, BAO and HST data are significantly higher than three which ensures the larger best-fit values of the Hubble parameter. The  $H_0$  values obtained in the analysis of cosmological model having self-interacting neutrinos with Planck CMB, BAO and HST data reaches to the value of  $H_0$  obtained from HST measurement. However, for this model, the  $H_0$  inferred from the Planck CMB data alone does not change much from the  $H_0$  values obtained in the  $\Lambda\text{CDM}$  model.

Next, we test the flavour specific interactions with IceCube. It has been pointed out that PeV neutrinos from astrophysical sources can interact with cosmic neutrinos and produce an on shell mediator  $\nu\nu \rightarrow \phi$ , when the neutrino energy  $E_\nu = m_\phi^2/(2m_\nu)$  and neutrino self-interactions with MeV mass mediators can have a signature in the neutrino spectrum observed at IceCube [15, 17, 26–30]. The resonant absorption of astrophysical neutrinos will show up as dips in the IceCube flux and this may explain the gap in the IceCube observations between  $E_\nu = 400 \text{ TeV} - 1 \text{ PeV}$ <sup>1</sup>. Since the neutrino interactions are defined in the flavour basis while the resonance is in the mass basis, the neutrino mixing angles and mass hierarchies also play a crucial role in the IceCube spectrum. We find that all the flavour specific interactions show similar pattern in the IceCube flux data, although these patterns are highly different from the universal interaction. We also find that, for the flavour specific and the universal self-interaction, the cosmological allowed SI region of interaction is ruled out by IceCube data while the MI region is partially consistent with IceCube for both the inverted and normal neutrino mass hierarchies.

The paper is organised as follows. In Section 2 we discuss the models of flavour specific self-interactions and discuss the scattering cross-section in the low energy limit relevant for CMB anisotropy, neutrino free-streaming and the high energy resonant interactions which are relevant for IceCube neutrinos. In Section 3 we discuss the constraints on effective interaction strength ( $G_{\text{eff}}$ ) for the flavour specific and universal interactions from Planck CMB, BAO

---

<sup>1</sup>Very recently, the IceCube collaboration has reported the observation of Glashow-resonance event at  $E_\nu = 6.3 \text{ PeV}$  [31]. When we were doing the analysis for this work. There was no observation of the Glashow resonance; that is why we have not used that in this work. However, we plan to include this in future analyses.

and HST data. In Section 4 we discuss the propagation of high energy neutrinos in cosmic neutrino background with resonant scattering. In Section 5 we apply the analysis of high energy neutrino propagation to IceCube flux considering the four flavour specific neutrino interactions for the two mass hierarchies. In Section 6, we conclude the viability of neutrino interaction models in the light of cosmological and IceCube data.

## 2 Self-interaction in neutrinos

Neutrino self-interactions can be mediated by scalars and gauge bosons which are motivated from different particle physics models[32–37]. The lepton number is conserved in the standard model and in the extensions of the standard model where lepton number is broken spontaneously, there are scalars called Majorons which arise from Goldstone bosons of the lepton number symmetry breaking [38]. Neutrino self-interactions can also arise from the gauged lepton number and anomaly free extensions of the standard model where light gauge bosons couple to the neutrinos and evade all other experimental constraints [39]. To analyse the low energy particle physics and CMB constraints, it is enough to work in the effective theory framework [24]. However, to analyse high energy IceCube interactions, where the resonance behaviour of cross-section is needed, the full theory is required.

The neutrino self-interactions are defined in the flavour basis ( $\nu_\alpha$ ) but the high energy propagation and the neutrino free-streaming is analysed in the neutrino mass basis ( $\nu_i$ ). Here Greek letters are for three different flavours  $e, \mu$  and  $\tau$  and Latin letters are for mass eigenstates which run from 1 to 3. To relate the couplings in the flavour basis to those in the mass basis, the PMNS mixing matrix defined as

$$|\nu_\alpha\rangle = U_{\alpha i}|\nu_i\rangle, \quad (2.1)$$

where the values of the components of  $U_{\alpha i}$  have been taken from latest NuFit data [40]. Global analysis of the latest neutrino oscillation data provides us the values for all the oscillation parameters like mass squared difference  $\Delta m_{ij}^2 = m_i^2 - m_j^2$  and the mixing angles. However, the existing data failed to give the correct sign of  $\Delta m_{31}^2$  or  $\Delta m_{32}^2$ . Therefore, we have two mass hierarchies, namely normal hierarchy (NH) and inverted hierarchy (IH). In case of NH  $m_1 < m_2 < m_3$  and in case of IH  $m_3 < m_1 < m_2$ . For both the hierarchies, we will assume the lowest neutrino mass to be  $m_0$ .

Self-interaction in between the active neutrino species can occur from gauge-interaction or Yukawa like interactions mediated by a scalar( $\phi$ ) particle. In case of Yukawa like interactions the Lagrangian can be written as

$$-\mathcal{L} = g_\phi \sum_{\alpha, \beta} g_{\alpha\beta} \phi \bar{\nu}_\alpha \nu_\beta, \quad (2.2)$$

where  $g_\phi$  is the coupling strength. In the mass basis this can be written as

$$-\mathcal{L} = g_\phi \sum_{i, j} g_{ij} \phi \bar{\nu}_i \nu_j, \quad (2.3)$$

where  $g_{ij} = g_{\alpha\beta} U_{\alpha i}^* U_{\beta j}$ . Similarly for gauge-interactions the Lagrangian can be written as

$$-\mathcal{L} = g_X \sum_{\alpha, \beta} \bar{\nu}_\alpha g_{\alpha\beta} \gamma^\mu P_L \nu_\beta X_\mu, \quad (2.4)$$

where  $g_X$  is the coupling strength. In terms of mass eigenstates this kind of interaction term becomes

$$-\mathcal{L} = g_X \sum_{i,j} g_{ij} \bar{\nu}_i \gamma^\mu P_L \nu_j X_\mu. \quad (2.5)$$

The matrix  $g_{\alpha\beta}$  defines the flavour dependence of the interactions. As discussed earlier, in this paper, we will work with four different types of flavour dependencies. Therefore  $g_{\alpha\beta}$  will be  $\delta_{\alpha\beta}$  for universal interaction and for interaction in a particular flavour it will be a diagonal matrix with only one among  $g_{ee}, g_{\mu\mu}$  or  $g_{\tau\tau}$  set to be one.

For both the scalar and vector exchange cases, for momentum-transferred smaller than the mediator mass, the neutrino self-interactions can be described by the four-Fermi term

$$\mathcal{L} = G_{\text{eff}} g_{\alpha\beta} g_{\gamma\delta} \bar{\nu}_\alpha \nu_\beta \bar{\nu}_\gamma \nu_\delta, \quad (2.6)$$

where  $G_{\text{eff}} = g_\phi^2/m_\phi^2$  or  $G_{\text{eff}} = g_X^2/m_X^2$  for scalar and gauge boson exchange respectively. In the mass basis, the above Lagrangian takes the following form:

$$\mathcal{L} = G_{\text{eff}} g_{ij} g_{kl} \bar{\nu}_i \nu_j \bar{\nu}_k \nu_l. \quad (2.7)$$

Therefore, for a process like  $\bar{\nu}_i \nu_j \rightarrow \bar{\nu}_k \nu_l$ , the cross-section will be given as  $\sigma_{ijkl} = |g_{kl}|^2 |g_{ij}|^2 G_{\text{eff}}^2$ . After summing over the final states, the cross-section is given as

$$\sigma_{ij} = \sum_{k,l} |g_{kl}|^2 |g_{ij}|^2 G_{\text{eff}}^2 = \mathcal{A} |g_{ij}|^2 G_{\text{eff}}^2, \quad (2.8)$$

where  $\mathcal{A} = \sum_{k,l} |g_{kl}|^2$ . For a diagonal  $g_{\alpha\beta}$  considered in this work,  $\mathcal{A} = \sum_{k,l} U_{k\alpha}^\dagger g_{\alpha\beta} U_{\beta l}$ . For the CMB analysis where the momentum transfer in neutrino scatterings are smaller than  $\text{MeV}^2$ , the Four-Fermi effective operator is adequate for the analysis. However, when we consider interactions of high-energy astrophysical neutrinos with the cosmic neutrino background, the effective Four-Fermi interaction is not applicable and one must do the calculations for the full theory with the mediator mass playing a crucial role specially near resonant scattering energies. The high energy neutrino-neutrino scattering cross-section due to scalar exchange is given by [30, 41, 42]

$$\sigma_{ijkl} = \sigma(\bar{\nu}_i \nu_j \rightarrow \bar{\nu}_k \nu_l) = \frac{1}{4\pi} |g_{kl}|^2 |g_{ij}|^2 \frac{g_\phi^4 s_j}{(s_j - m_\phi^2)^2 + m_\phi^2 \Gamma_\phi^2}, \quad (2.9)$$

where  $s_i = 2E_i m_i$  and  $\Gamma_\phi = g_\phi^2 \sum_{i,j} |g_{ij}|^2 m_\phi / 4\pi$  is the decay width of the mediator. For vector interactions the cross-section has the same Breit-Wigner form with different constants in the prefactor. When summed over the final states this turns out to be

$$\sigma_{ij} = \sigma(\bar{\nu}_i \nu_j \rightarrow \bar{\nu} \nu) = \sum_{k,l} \sigma_{ijkl}. \quad (2.10)$$

Therefore, we can see that for those energies where  $s_i$  becomes equal to the  $m_\phi^2$ , the scattering cross-section becomes maximum. These energies are called resonant energies and denoted by  $E_{Ri} = m_\phi^2 / 2m_i$ . In section 4 we will show that corresponding to these resonant energies the absorption rates of astrophysical neutrinos reach the maximum value and we find the dips in the neutrino spectrum in those energy values.

### 3 Constraints from cosmological data set

We now turn our focus on the cosmological perturbation theory in the presence of self-interaction in massive neutrinos. Massive neutrinos play an important role in the evolution of cosmological perturbations as well as in the evolution of background cosmology. Generally, neutrinos free stream in the baryon-photon fluid of early universe and their free streaming length mainly depends on their masses. However, if the neutrinos have self-interaction in between them then that reduces their free streaming length and makes the neutrinos clump together more and more than the free neutrinos. The mass of the neutrinos on the other hand not only modifies the free streaming length but also modifies the Hubble parameter. That is why the effects of self-interacting neutrinos and the massive neutrinos on CMB are not same. The neutrino interactions are defined in the flavour basis while the neutrino density perturbations are analysed in the mass basis. To study this, we need to calculate the density matrix for the neutrinos which can be written as  $\rho_{\alpha\beta} = |\nu_\alpha\rangle\langle\nu_\beta|$  and this transforms to mass basis as

$$\rho_{\alpha\beta} = U_{\alpha i} \rho_{ij} U_{j\beta}^* . \quad (3.1)$$

Next, we need to find out the Boltzmann hierarchy equations for the massive neutrinos in the presence of a collision term arising due to the self-interacting neutrinos, which can be written as [43]

$$\frac{\partial \Psi_i}{\partial \tau} + i \frac{q(\vec{k} \cdot \hat{n})}{\epsilon} \Psi_i + \frac{d \ln f_0}{d \ln q} \left[ \dot{\eta} - \frac{\dot{h} + 6\dot{\eta}}{2} (\hat{k} \cdot \hat{n})^2 \right] = \frac{1}{\bar{f}_0^i} \frac{\partial f_i}{\partial \tau} \quad (3.2)$$

where  $\bar{f}_0^i = \sum_\alpha f_0 |U_{\alpha i}|^2 \rho_{\alpha\alpha}$  with  $f_0$  being the zeroth order Fermi-Dirac distribution function [6], and  $\Psi$  is the scalar perturbation in the distribution function. If there is no self-interaction, the collision term on the right hand side of this equation will be set to zero. The scalar perturbation  $\Psi$  in the distribution function is expanded in terms of the Legendre polynomials as,

$$\Psi(\vec{k}, \hat{n}, q, \tau) = \sum_{\ell=0}^{\infty} (-i)^\ell (2\ell + 1) \Psi_\ell(\vec{k}, q, \tau) P_\ell(\hat{k} \cdot \hat{n}) . \quad (3.3)$$

Such expansion of  $\Psi$  leads to the Boltzmann hierarchy equations consisting of the individual equations corresponding to each multipole.

The collision term for the Boltzmann hierarchy equations in the case of neutrino has been considered in literature in many different ways. Refs. [2, 3, 44] provide the exact calculation, refs. [45, 46] provide the effective fluid equation and refs. [1, 6, 47] obtain the collision term under the relaxation time approximation. We follow the relaxation time approximation since it is computationally less time taking. According to relaxation time approximation the collision term with  $\ell \geq 2$  is given as

$$\frac{1}{\bar{f}_0^i} \frac{\partial f_i}{\partial \tau} = -\Gamma_{ij} \Psi_j . \quad (3.4)$$

Here  $\Gamma_{ij}$  is the scattering rate between neutrinos, which is defined as

$$\Gamma_{ij} = an_\nu \langle \sigma_{ij} v \rangle \quad (3.5)$$

where  $\sigma_{ij} = \mathcal{A} |g_{ij}|^2 G_{\text{eff}}^2 T_\nu^2$  is the effective cross-section for the self-interacting neutrinos on the CMB relevant scales (see eq. (2.8)). For a diagonal matrix  $g_{\alpha\beta}$  as considered in this paper,

$|g_{ij}|^2 = U_{i\alpha}^\dagger g_{\alpha\beta} U_{\beta j}$ . Therefore, the scattering rate can be written as

$$\Gamma_{ij} = U_{i\alpha}^\dagger g_{\alpha\beta} U_{\beta j} \frac{3}{2} \frac{\zeta(3)}{\pi^2} a G_{\text{eff}}^2 T_\nu^5 \rho_{kk} \mathcal{A}, \quad (3.6)$$

where we have assumed the neutrino temperature ( $T_\nu$ ) to remain the same for the three neutrino mass eigenstates in the presence of self-interaction. Here, the diagonal elements of the neutrino density matrix  $\rho_{kk}$  correspond to the neutrino number density  $n_\nu$  normalized to the number density  $n_\nu^*$  in a reference model, which is assumed to be the  $\Lambda$ CDM model plus three active neutrinos without self-interaction [47]. As a result, a factor of  $\rho_{kk}$  arises in the scattering rate. However, this factor is unimportant here as it is equal to one in this case. But, as shown in ref. [6, 47], the value of this factor deviates from one in the case of self-interacting light sterile neutrinos. Let us now rewrite the scattering rate in the relaxing time approximation as [48]

$$\Gamma_{ij} = U_{i\alpha}^\dagger g_{\alpha\beta} U_{\beta j} \tau_\nu^{-1} \quad \text{with} \quad \tau_\nu^{-1} = \frac{3}{2} \frac{\zeta(3)}{\pi^2} a G_{\text{eff}}^2 T_\nu^5 \rho_{kk} \mathcal{A}, \quad (3.7)$$

However, the exact form of collision term for  $\ell = 0$  and  $\ell = 1$  in relaxation time approximation for self-interaction in different species are not available in literature. Therefore we move forward here with the following assumptions. According to ref. [44], the exact collision term in  $\ell = 0$  and  $\ell = 1$  equations depends on the differences between the distribution functions of different mass eigenstates. Let us investigate if that term would have any significant contribution. The  $G_{\text{eff}}$  values allowed from CMB data has been reported to be less than  $\sim 10^{-1} \text{ MeV}^{-2}$  [3]. For this level of interaction we find that the self-interaction rate of the neutrinos becomes smaller than the Hubble expansion rate at a temperature  $T \sim 20 \text{ eV}$ . However, neutrino masses that we will consider in this paper will be limited to less than 1 eV. Therefore, when the self interaction plays its role in Boltzmann equations, the neutrinos will be completely in the relativistic regime and they will have the same distribution function for all the mass eigen states. Moreover, we have already considered that the neutrinos are in thermal equilibrium with each other which ensures that number of each species should be conserved. Therefore we set collision term to zero in  $\ell = 0$  case. However, there can be a velocity slip kind of term in the equation for  $\ell = 1$  for conservation of overall momentum. Such an term will introduce a term like  $\Gamma_{ij}(\Psi_{j,1} - \Psi_{i,1})$  in the equation for  $\ell = 1$  for our case. We checked the effect of such a term on the CMB power spectrum and found it to be indistinguishable from the power spectrum where this term is not considered. Therefore, for doing the MCMC analysis, we set this term to zero. In a very recent study similar assumption is taken by setting the neutrino masses to zero [49].

Using Eqs. (3.7) and (3.4) in eq. (3.2) and eq. (3.3) the Boltzmann hierarchy equations takes the following form [47, 50]

$$\dot{\Psi}_{i,0} = -\frac{qk}{\epsilon} \Psi_{i,1} + \frac{1}{6} \dot{h} \frac{d \ln f_0}{d \ln q}, \quad (3.8a)$$

$$\dot{\Psi}_{i,1} = \frac{qk}{3\epsilon} (\Psi_{i,0} - 2\Psi_{i,2}), \quad (3.8b)$$

$$\dot{\Psi}_{i,2} = \frac{qk}{5\epsilon} (2\Psi_{i,1} - 3\Psi_{i,3}) - \left( \frac{1}{15} \dot{h} + \frac{2}{5} \dot{\eta} \right) \frac{d \ln f_0}{d \ln q} - \Gamma_{ij} \Psi_{j,2}, \quad (3.8c)$$

$$\dot{\Psi}_{i,\ell} = \frac{qk}{(2\ell+1)\epsilon} \left[ \ell \Psi_{i,(\ell-1)} - (\ell+1) \Psi_{i,(\ell+1)} \right] - \Gamma_{ij} \Psi_{j,\ell} \quad (\ell \geq 3). \quad (3.8d)$$



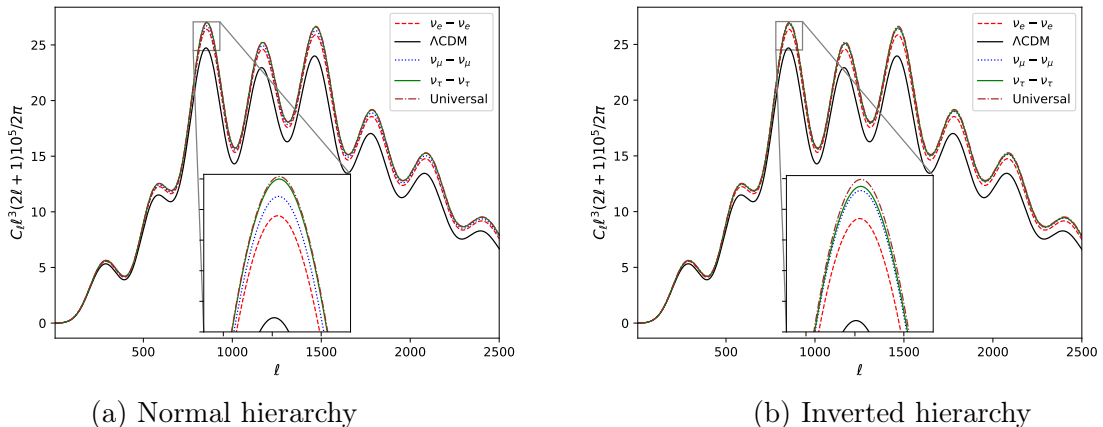


**Figure 1:** Effects of flavour specific interactions on CMB temperature power spectrum are shown. Power spectrum corresponding to universal interaction almost overlaps with that of  $\nu_\tau$ - $\nu_\tau$  interaction for both the hierarchies. The value of  $G_{\text{eff}}$  has been fixed to  $10^{-1.5}\text{MeV}^{-2}$  for all these cases.

We modified these equations (eq. (3.8)) accordingly in the Boltzmann code CLASS [51] and have shown the effects of these interactions on CMB in fig. (1). In general, self-interaction between neutrinos helps the small scale perturbations to grow therefore the height of the peaks in CMB power spectrum increases. However, the effect of flavour specific interactions on CMB spectrum shows that there are some minor differences between the effects of different interactions. These effects can be understood from the equations 3.8. In the case of universal interaction when  $g_{\alpha\beta}$  is equal to  $\delta_{\alpha\beta}$  the  $\Gamma_{ij}$  becomes a diagonal matrix. That means the growth of the scalar perturbation multipoles ( $\Psi_\ell$ ) of one mass eigenstate depends only on that mass eigenstate. However, for the case of flavour specific interactions growth of  $\Psi_\ell$  depends on other mass eigenstates too. Ultimately, the amount of the effect of self-interaction is determined by the quantity  $\sum_{i,j} \Gamma_{ij}$ . In case of universal interaction it is  $3\tau_\nu^{-1}$ . For  $\nu_e$ - $\nu_e$  interaction this becomes  $2.308 \tau_\nu^{-1}$ , for  $\nu_\mu$ - $\nu_\mu$   $2.643 \tau_\nu^{-1}$  and for  $\nu_\tau$ - $\nu_\tau$  it turns out to be  $2.965 \tau_\nu^{-1}$ . In case of inverted hierarchy these numbers are  $2.309 \tau_\nu^{-1}$  for  $\nu_e$ - $\nu_e$ ,  $2.809 \tau_\nu^{-1}$  for  $\nu_\mu$ - $\nu_\mu$  and  $2.88116 \tau_\nu^{-1}$  for  $\nu_\tau$ - $\nu_\tau$ . Therefore, we see that the effects of universal interaction and  $\nu_\tau$ - $\nu_\tau$  interaction on CMB are almost indistinguishable for both the hierarchies in fig. (1).

We proceed to constrain the parameter space of  $G_{\text{eff}}$  with Markov Chain Monte Carlo (MCMC) technique using MontePython [52]. We have used the Planck high- $\ell$  and low- $\ell$  likelihood, following ref [18, 53] where high- $\ell$  consists of only  $TT$  spectrum and  $TT, TE$  and  $EE$  spectrum is incorporated in low- $\ell$  likelihood<sup>2</sup>. We have used two other data sets. One is baryon acoustic oscillation scale set by BAO-BOSS data of DR12 release [54] and another one

<sup>2</sup>In the literature, the high- $\ell$  polarization data have also been used to constrain neutrino self-interaction. However, we have only used high and low- $\ell$  data for temperature anisotropy and low- $\ell$  polarization data to be consistent with our previous work [6] and to avoid extra computational time. The constrained value of  $G_{\text{eff}}$  obtained in our analysis is similar to the value found in other analyses where high- $\ell$  polarization is used. In this work, our main focus is to compare the  $G_{\text{eff}}$  values allowed from the cosmological observations with the best-fit values of the IceCube observation. Inclusion of high- $\ell$  polarization data may change the allowed  $G_{\text{eff}}$  values slightly, however, the conclusion of this work will not be affected by it.



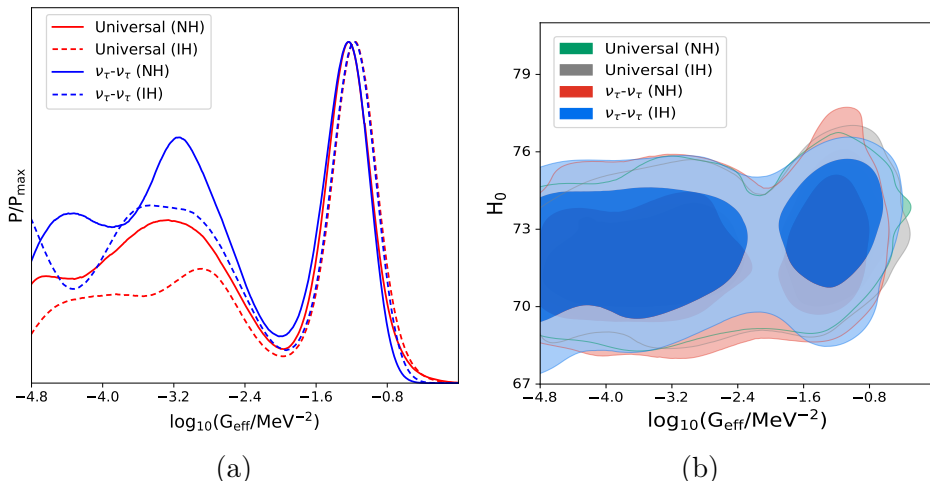


**Figure 2:** (a) Posterior distribution of  $G_{\text{eff}}$  is bimodal in nature. (b) Inclusion of self-interaction leads to higher  $H_0$  as compared to that in  $\Lambda$ CDM model with  $N_{\text{eff}}$  greater than three when Planck, BAO and HST data analysed jointly. There is no significant effect of hierarchies or the flavour specific nature of the self-interaction on constraining parameters.

is the measured value of  $H_0$  by Hubble space telescope from the observations of Cepheid [23]. We will refer this combined data set as “Planck+BAO+HST”. In this analysis we have varied  $N_{\text{eff}}$ , lowest neutrino mass  $m_0$  and six standard cosmological parameters. The details of the MCMC analysis is provided in the appendix A.

Parameter	Universal Interaction (NH)	Universal Interaction (IH)	$\nu_\tau$ - $\nu_\tau$ Interaction (NH)	$\nu_\tau$ - $\nu_\tau$ Interaction (IH)
$10^2 \omega_b$	$2.269^{+0.037}_{-0.033}$	$2.268 \pm 0.036$	$2.261 \pm 0.037$	$2.267 \pm 0.034$
$\omega_{\text{cdm}}$	$0.1286^{+0.0058}_{-0.0068}$	$0.1286 \pm 0.0059$	$0.1279^{+0.0051}_{-0.0060}$	$0.1281^{+0.0054}_{-0.0065}$
$100\theta_s$	$1.0412^{+0.0009}_{-0.0011}$	$1.0411^{+0.0010}_{-0.0013}$	$1.0413^{+0.0010}_{-0.0011}$	$1.0411 \pm 0.0010$
$\ln(10^{10} A_s)$	$3.062 \pm 0.038$	$3.062 \pm 0.037$	$3.058 \pm 0.037$	$3.056 \pm 0.035$
$n_s$	$0.987 \pm 0.014$	$0.988^{+0.016}_{-0.013}$	$0.984^{+0.016}_{-0.013}$	$0.987 \pm 0.014$
$\tau_{\text{reio}}$	$0.057 \pm 0.016$	$0.058 \pm 0.016$	$0.056 \pm 0.016$	$0.055 \pm 0.016$
$m_0$	$0.058^{+0.022}_{-0.051}$	$0.059^{+0.024}_{-0.056}$	$0.052^{+0.018}_{-0.049}$	$0.053^{+0.019}_{-0.044}$
$\log_{10} G_{\text{eff}}$	$-3.48^{+0.94}_{-0.65}$	$-3.47^{+0.79}_{-0.75}$	$-3.44^{+1.0}_{-0.63}$	$-3.56^{+1.1}_{-0.79}$
$N_{\text{eff}}$	$3.76^{+0.31}_{-0.38}$	$3.78^{+0.29}_{-0.34}$	$3.69^{+0.29}_{-0.33}$	$3.75 \pm 0.33$
$H_0$	$72.0^{+1.7}_{-1.9}$	$71.9 \pm 1.7$	$71.6 \pm 1.7$	$71.9^{+2.0}_{-1.8}$

**Table 1:**  $1-\sigma$  allowed values of all the parameters for the moderate self-interaction (MI) for both universal and  $\nu_\tau$ - $\nu_\tau$  interactions.

As shown in the earlier literature [1–3] we also find that the Planck data along with BAO and HST data prefer a small region of strong interaction between the neutrinos in fig. (2)-(a). The posterior of  $G_{\text{eff}}$  is bi-modal. For quantifying the two regions of self-interaction we separate out the points from the posterior distribution which have  $\log_{10}(G_{\text{eff}})$  values greater than -1.95 and less than that. We use GetDist [55] to extract the statistics of these peaks. The strong interaction region (we call SI onwards) has the value of  $\log_{10}(G_{\text{eff}}/\text{MeV}^{-2})$  in one sigma range as  $-1.25^{+0.21}_{-0.18}$  for universal interaction in the normal hierarchy,  $-1.17 \pm 0.23$  for universal interaction in the inverted hierarchy,  $-1.28^{+0.26}_{-0.17}$  for  $\nu_\tau$ - $\nu_\tau$  interaction in the normal hierarchy and  $-1.18^{+0.17}_{-0.12}$  for  $\nu_\tau$ - $\nu_\tau$  interaction in the inverted hierarchy. For these

Parameter	Universal Interaction (NH)	Universal Interaction (IH)	$\nu_\tau$ - $\nu_\tau$ Interaction (NH)	$\nu_\tau$ - $\nu_\tau$ Interaction (IH)
$10^2 \omega_b$	$2.237 \pm 0.036$	$2.249 \pm 0.035$	$2.246 \pm 0.041$	$2.250 \pm 0.035$
$\omega_{cdm}$	$0.1344 \pm 0.0064$	$0.1349 \pm 0.0066$	$0.1369^{+0.0073}_{-0.0063}$	$0.1371^{+0.0078}_{-0.0047}$
$100\theta_s$	$1.0457 \pm 0.0012$	$1.0455^{+0.0011}_{-0.0014}$	$1.0453 \pm 0.0011$	$1.0451^{+0.0009}_{-0.0010}$
$\ln(10^{10} A_s)$	$3.002 \pm 0.039$	$3.003^{+0.031}_{-0.037}$	$3.002 \pm 0.036$	$3.012 \pm 0.035$
$n_s$	$0.958 \pm 0.014$	$0.959 \pm 0.013$	$0.961 \pm 0.013$	$0.964 \pm 0.011$
$\tau_{reio}$	$0.054 \pm 0.016$	$0.055^{+0.013}_{-0.015}$	$0.049 \pm 0.016$	$0.054 \pm 0.015$
$m_0$	$0.080^{+0.039}_{-0.068}$	$0.083^{+0.043}_{-0.053}$	$0.083^{+0.043}_{-0.061}$	$0.091^{+0.062}_{-0.063}$
$\log_{10} G_{\text{eff}}$	$-1.25^{+0.21}_{-0.18}$	$-1.17 \pm 0.23$	$-1.28^{+0.26}_{-0.17}$	$-1.18^{+0.17}_{-0.12}$
$N_{\text{eff}}$	$3.93 \pm 0.35$	$3.98 \pm 0.36$	$4.06 \pm 0.35$	$4.10^{+0.39}_{-0.19}$
$H_0$	$72.7 \pm 1.9$	$72.9 \pm 1.7$	$73.3 \pm 1.8$	$73.2 \pm 1.8$

**Table 2:** 1- $\sigma$  allowed values of all the parameters for the strong self-interaction (**SI**) for both universal and  $\nu_\tau$ - $\nu_\tau$  interactions.

specific interactions the bestfit values for  $\log_{10}(G_{\text{eff}}/\text{MeV}^{-2})$  in the mildly interacting region (we call MI onwards) are  $-3.48^{+0.94}_{-0.65}$ ,  $-3.47^{+0.79}_{-0.75}$ ,  $-3.44^{+1.0}_{-0.63}$  and  $-3.56^{+1.1}_{-0.79}$  respectively. The combined ‘‘Planck+BAO+HST’’ analysis in the case of varying  $N_{\text{eff}}$  can push the value of  $H_0$  up to  $73.3 \pm 1.8$  in the case of  $\nu_\tau$ - $\nu_\tau$  interaction in normal hierarchy. Similarly for other interactions also the best-fit value of  $H_0$  becomes higher (see fig. (2)-(b)). Values of all other parameters are presented in table 1 and table 2.

In fig. (1) we see that difference in between different types of interactions is almost indistinguishable unless magnified. Even after magnification there is almost no difference in between the effects of  $\nu_\tau$ - $\nu_\tau$  and universal interaction on CMB spectra. Similarly the MCMC bound on  $G_{\text{eff}}$  for the universal interaction are almost same to the bound in  $\nu_\tau$ - $\nu_\tau$  interaction for both the hierarchies. With these bounds on  $G_{\text{eff}}$  and  $m_0$  in hand we move forward to calculate the effect of neutrino self-interactions on IceCube flux.

## 4 Neutrino absorption by Cosmic Neutrino Background

Propagation of the astrophysical neutrinos in the cosmic neutrino background can be described by the Boltzmann equation. The specific flux  $\Phi_i$  of neutrino mass eigenstates  $m_i$  is defined as

$$\Phi_i = \frac{\partial n_i}{\partial E}, \quad (4.1)$$

where  $n_i$  is the comoving number density of the astrophysical neutrinos per unit time and  $E$  is the energy of the neutrino mass eigenstates. Therefore, the unit of the  $\Phi_i$  is  $\text{cm}^{-2}\text{s}^{-1}\text{sr}^{-1}\text{eV}^{-1}$ . The Boltzmann equation for  $\Phi_i$  is defined as [14, 42]

$$\frac{\partial \Phi_i}{\partial t} = H\Phi_i + HE\frac{\partial \Phi_i}{\partial E} + S_i(t, E) - \Gamma_i(t, E)\Phi_i + S_{\text{tert},i}(t, E). \quad (4.2)$$

Here,  $H$  denotes the Hubble parameter,  $S_i$  is the source term of the astrophysical neutrinos,  $\Gamma_i$  is absorption rate and  $S_{\text{tert},i}$  is the tertiary source term. Absorption rate  $\Gamma_i = \sum_j \tilde{n}_j \sigma_{ij}$ , where  $\tilde{n}_j$  is the comoving cosmological neutrino number density [30]. Absorption rate is plotted against energy in fig. (3), we can see that  $\Gamma_i$  becomes maximum at the resonance energies. For solving eq. (4.2), we recast it in redshift ( $z$ ) variable as

$$(1+z)\frac{\partial \Phi_i}{\partial z} + E\frac{\partial \Phi_i}{\partial E} = -\Phi_i - \frac{S_i(z, E)}{H} + \frac{\Gamma_i(z, E)}{H}\Phi_i - \frac{S_{\text{tert},i}(z, E)}{H}. \quad (4.3)$$

Solution of this equation is done using method of auxiliary equation [14, 42], where the auxiliary equation is set to be

$$E = E_0(1 + z). \quad (4.4)$$

Here  $E_0$  denotes the energy of neutrinos at  $z = 0$ . The solution of eq. (4.3) can be written as [56]

$$\Phi_i(E_0, z) = \int_0^\infty \frac{dz'}{H(z')} \exp \left[ \int_z^{z'} \frac{dz''}{(1+z'')} \frac{\Gamma_i(E, z'')}{H(z'')} \right] \{S_i(E, z) + S_{\text{tert},i}(E, z)\}. \quad (4.5)$$

As proposed in the literature, there can be many possible astrophysical sources for the high-energy neutrinos, which power the source term  $S_i$ . For example, gamma-ray blazars [57–61], gamma-ray bursts [62–68], Radio-bright AGN [69], choked jet supernovae [70, 71], pulsar wind nebulae [72], etc. However, it is still unclear about the exact source of these high energy neutrinos. All these different sources can have different spectra for the neutrino flux. As an example, the source term related to the core-collapsed supernova (CCSN) reads as [73]

$$S_i(E, z) = R_{\text{CCSN}}(z) \frac{dN_i}{dE} E^{-\gamma_c}, \quad (4.6)$$

where  $\frac{dN_i}{dE}$  is the comoving neutrino production rate per unit time per unit energy, and it is defined as

$$\frac{dN_i}{dE} = \frac{120E^2 E_{\text{tot}}}{(7\pi^2) 6(k_B T_{\text{sn}})^4 (e^{E/k_B T_{\text{sn}}} + 1)}, \quad (4.7)$$

where  $E_{\text{tot}} = 1.873 \times 10^{65} \text{eV}$  and  $k_B T_{\text{sn}} = 8 \text{MeV}$  [30]. It is evident from eq. (4) that the neutrino flux coming from CCSN will peak in the  $\mathcal{O}(10)$  MeV range. Therefore, the CCSN can not produce a significant flux of ultra-high energy neutrinos relevant to the IceCube energy range. However, as argued in ref.[30], the redshift distribution of the ultra high energy neutrino sources is expected to closely follow the  $R_{\text{CCSN}}(z)$ . Therefore, we have considered the source term  $S_i$  at the IceCube relevant energy range to be an effective power law as

$$S_i(E, z) \propto R_{\text{CCSN}}(z) \left( \frac{E}{E_0} \right)^{-\gamma}. \quad (4.8)$$

Later in this section, we fix the normalization of the neutrino flux with the observed flux at 100 TeV.

$R_{\text{CCSN}}(z)$  represents the number density of the core-collapsed supernova as a function of  $z$ . We take this function from ref [74]

$$R_{\text{CCSN}}(z) = \dot{\rho} \left( \left( \frac{z+1}{B} \right)^{\beta\eta} + \left( \frac{z+1}{C} \right)^{\gamma_2\eta} + (z+1)^{\alpha\eta} \right)^{1/\eta} \quad (4.9)$$

with the parameters being  $\dot{\rho} = 0.0178$ ,  $z_1 = 1$ ,  $z_2 = 4$ ,  $\alpha = 3.4$ ,  $\beta = -0.3$ ,  $\gamma_2 = -3.5$ ,  $\eta = -10$ ,  $B = (z_1 + 1)^{1-\frac{\alpha}{\beta}}$  and  $C = (z_2 + 1)^{1-\frac{\beta}{\gamma_2}} (z_1 + 1)^{\frac{\beta-\alpha}{\gamma_2}}$ .

Tertiary source term,  $S_{\text{tert},i}$  accounts for the up-scattering of the cosmological neutrinos from the collision with astrophysical neutrinos. This term is approximated in the literature in many different ways. In this paper we use the form provided by ref [30] which is

$$S_{\text{tert},i}(z, E) = \sum_{jkl} (1 + \delta_{il}) \tilde{n}_k(z) \sigma_{jkil} \Phi_j(z, E_{R_k}) \Theta(E_{R_k} - E). \quad (4.10)$$

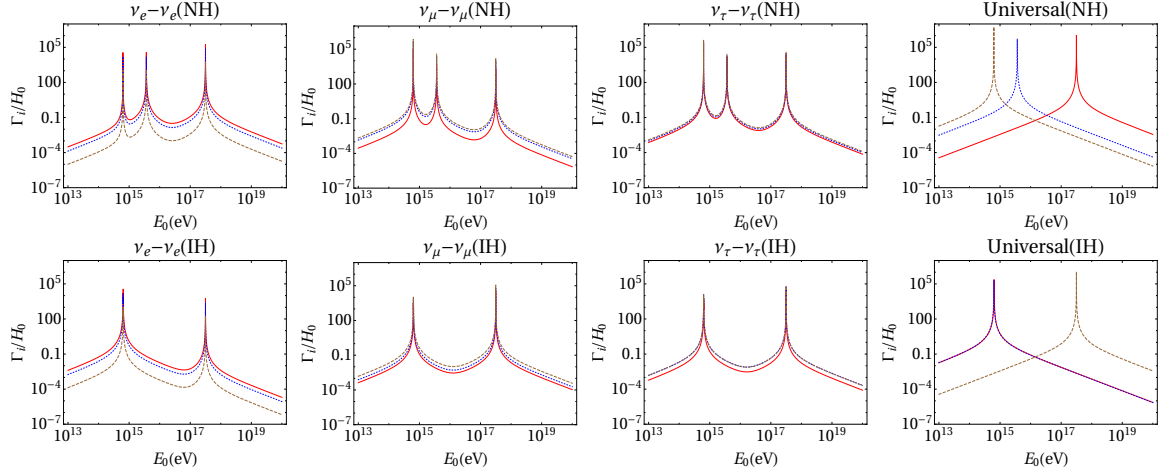


**Figure 3:** Effects of different types of interaction on absorption rate ( $\Gamma_i$ ) are shown. Red, blue (dotted) and brown (dashed) line demonstrate the interaction rates corresponding to mass eigenstates 1,2 and 3 respectively. Here, the upper panel represents normal hierarchy and the lower panel represents inverted hierarchy. Values of the parameters for these plots kept fixed at  $m_\phi = 10^{6.9}\text{eV}$ ,  $g_\phi = 10^{-1.5}$  and  $m_0 = 10^{-4}\text{eV}$ .

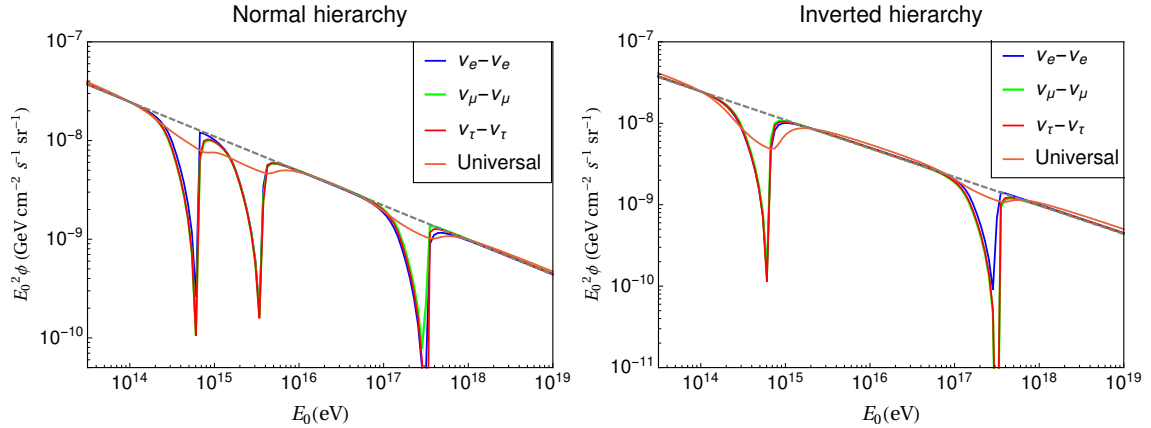


**Figure 4:** Effects of different types of self-interaction on total neutrino flux for both hierarchies are shown. Values of the parameters for these plots kept fixed at  $m_\phi = 10^{6.9}\text{eV}$ ,  $g_\phi = 10^{-1.5}$ ,  $\gamma = 2.35$  and  $m_0 = 10^{-4}\text{eV}$ . Dashed line corresponds to  $\Phi \propto E_0^{-\gamma}$ .

We have computed the specific flux of neutrino at  $z = 0$  by numerically solving eq. (4.5). We have taken the maximum value of  $z$  in this equation to be 10. It is because the  $R_{\text{CCSN}}(z)$  function has non-negligible value up to redshift ten. Normalization of the  $E_0^2 \sum_i \Phi_i$  is fixed to  $2.46 \times 10^{-8} \text{GeV cm}^{-2} \text{s}^{-1} \text{sr}^{-1}$  for neutrino energy equal to 100 TeV [75]. The results for different types of interactions and hierarchies are shown in fig. (4). To understand these plots we have made another set of plots in fig. (3) where the values of absorption rate,  $\Gamma_i$  has been plotted for different interactions. We see that there is a major difference between the universal interaction and the flavour specific interactions. In case of universal interaction the  $g_{ij}$  and  $g_{kl}$  in eq. (2.9) becomes kronekar delta function and thus  $\Gamma_i$  gets the contribution from  $s_i$  only. However, for flavour specific interactions  $g_{ij}$  mixes all the mass eigenstates

and  $s_j$  corresponding to all mass eigenstates contributes in  $\Gamma_i$ . Therefore, in fig. (3) we see that for flavour specific interactions the  $\Gamma_i$  shows resonance peaks in all three possible energy values corresponding to the three mass eigenstates in normal hierarchy. In the case of inverted hierarchy the mass gap between first two mass eigenstates are small, and the peaks corresponding to those mass eigenstates are indistinguishable, therefore, only two peaks are separately visible. These peaks in  $\Gamma_i$  leads to the absorption dips in the flux of astrophysical neutrinos in fig. (4). Since, in the case of flavour specific interactions all mass eigenstates undergo absorption in all dips (three dips for NH and two dips for IH), we see that the total flux also shows dips in all the resonance energies. However, in the case universal interaction in which energy one mass eigenstate undergoes resonant absorption other mass eigenstates do not. Therefore, in fig. (4) the universal curve shows a more flat line. The three different peaks in the  $\Gamma_i$  of universal interaction can come close together if neutrino masses become degenerate. In that case a prominent dip will be visible in the total neutrino flux for universal interaction also. However, that means it requires a higher value lowest neutrino mass and in the next section we will check if that is consistent with CMB bound.

We found that the contribution of the tertiary source term compared to the core-collapse supernova source term is negligibly small. Moreover, it considerably increases the computation time. Therefore, for constraining the parameter space using IceCube data we neglect the tertiary term in the next section.

## 5 Parameter estimation from flux at IceCube

In IceCube six-year HESE data, 82 events passed the selection criterion of which two are coincident with atmospheric muons and left out. The best fit for single power law flux is [75]

$$E_0^2 \phi = (2.46 \pm 0.8) \times 10^{-8} \left( \frac{E_0}{100 \text{ TeV}} \right)^{-0.92} \text{ GeV cm}^{-2} \text{ s}^{-1} \text{ sr}^{-1}, \quad (5.1)$$

which has a softer spectral index than the 3-year ( $\gamma = 2.3$ ) as well as the 4-year ( $\gamma = 2.58$ ) data. These events are binned in 6 values of energy and for other values of energy where no events have been observed, an upper bounds on the neutrino flux have been provided. For fitting our numerical results of flux with the IceCube data we have solved eq. (4.5) for 63 different values of  $E_0$  which are equally spaced in log scale within  $E_0$ -range of first 7 points in IceCube data (see fig. (5)). Therefore, we have sampled each energy bin with 9 points in the log scale. The average of these 9 points are assigned as the theoretical prediction of neutrino flux. These theoretical predictions are then compared to the observational values of binned flux and the allowed parameter space ( $m_\phi$ ,  $g_\phi$ ,  $m_0$  and  $\gamma$ ) has been estimated using the MCMC technique with Metropolis-Hastings algorithm. Please refer to the appendix A for details.

Before moving forward to describe our findings for different types of interactions and hierarchies, let us briefly summarize the effects of different parameters on the features of the specific flux of neutrinos in IceCube . These effects can be listed as

- The higher value of  $m_\phi$  shifts the dips towards the higher values of neutrino energy.
- The higher values of lowest neutrino mass  $m_0$  make the difference between the neutrino masses smaller and thus make absorption dips come closer.
- In case of universal interaction higher  $m_0$  makes dips sharper and lower  $m_0$  makes the flux more flat.

- In general, higher values of  $m_0$  make the neutrinos heavier and therefore the dips move towards lower values of neutrino energy.
- Higher values of  $g_\phi$  make the dips sharper.
- $\gamma$  determines the slope of the flux line. The more  $\gamma$  becomes close to the value 2 the more the flux line becomes flat.

In the next subsections we will discuss our findings of MCMC analysis of parameter space for both the hierarchies and different types of interactions.

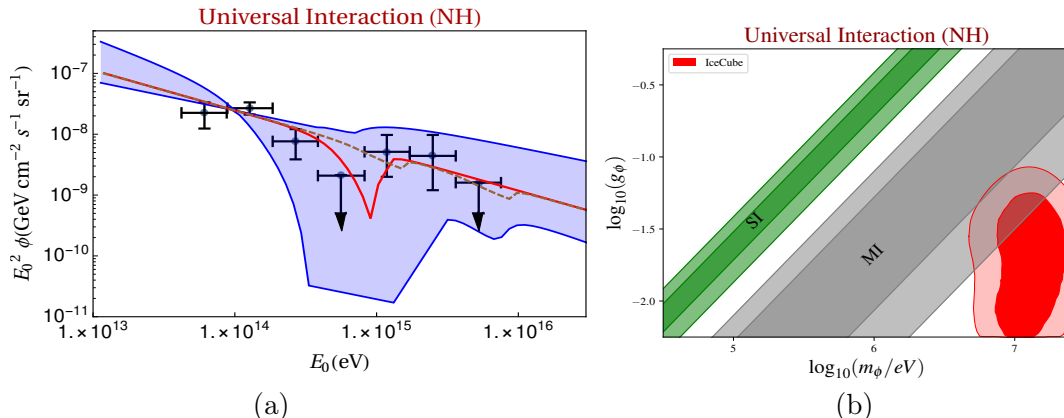


**Figure 5: Universal interaction in normal hierarchy:** (a) The shaded region corresponds to the specific flux of the neutrinos allowed by the 1- $\sigma$  ranges of all the parameters ( $m_\phi, g_\phi, \gamma$  and  $m_0$ ) as given in table 3. The solid red line corresponds to the bestfit values of all these parameters. However, the orange dashed line corresponds to parameters  $m_\phi, g_\phi$  and  $\gamma$  fixed at their bestfit values and  $m_0$  value fixed at zero. (b) The allowed 1- $\sigma$  and 2- $\sigma$  regions in the  $m_\phi$ - $g_\phi$  plane from IceCube data are shown along with the cosmological bound (“Planck+BAO+HST”) for universal interaction in the normal hierarchy. The allowed region for IceCube has no overlap with the strong self-interaction (SI) band.

## 5.1 Normal hierarchy

**Universal interactions:** Number of visible dips in the neutrino specific flux heavily depends on the value of the lowest neutrino mass  $m_0$ . Moreover, as shown in the fig. (4) the universal interaction produces more flat line of specific flux compared to the flavour specific interactions for smaller values of  $m_0$ . However, when the  $m_0$  is large, the absorption dips in flux lines corresponding to the different mass eigen states come closer and the dips in the total flux become sharper. Therefore, to fit the dips in the IceCube data the universal interaction prefers a higher value of  $m_0$ . The bestfit values along with 1- $\sigma$  error for all the parameters ( $m_\phi, g_\phi, \gamma$  and  $m_0$ ) are given in table 3. Moreover, the cosmological 1- $\sigma$  upper bound of  $m_0$  for the case of moderate universal interactions in the normal hierarchy is 0.079 eV (see table 1). The disallowed values of  $m_0$  are shown as the green shaded region in fig. (7)-(a). Therefore, It is clear from fig. (7)-(a) that a substantial region of the preferred mass range by IceCube is disallowed by the cosmological bound.

In fig. (5), the specific flux in IceCube and the corresponding allowed parameter space for  $m_\phi$ - $g_\phi$  have been shown. The shaded region in the fig. (5)-(a) corresponds to the specific

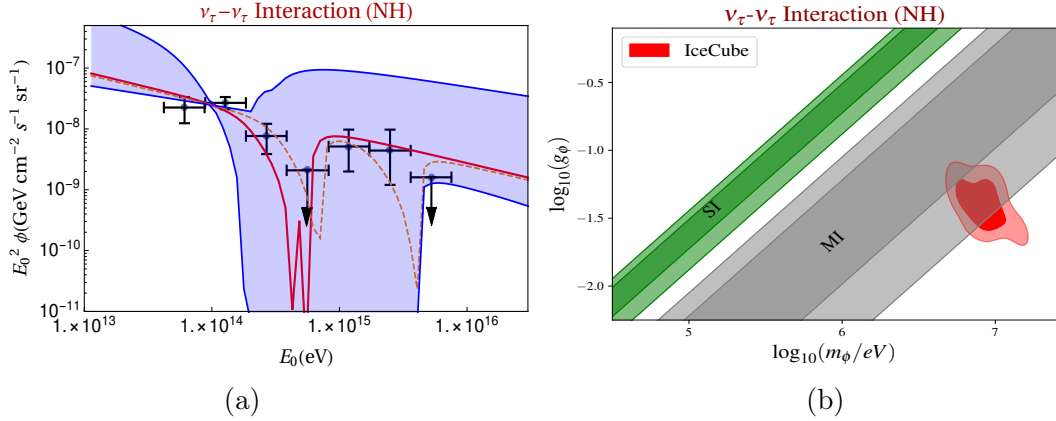


**Figure 6:  $\nu_\tau$ - $\nu_\tau$  interaction in normal hierarchy:** (a) The shaded region corresponds to the specific flux of the neutrinos allowed by the  $1\text{-}\sigma$  ranges of all the parameters in table 3. The solid red line correspond to the best fit values of all the parameters and the orange dashed line corresponds to the best fit value of  $m_\phi, g_\phi$  and  $\gamma$  and the value of  $m_0$  is fixed at zero. (b) The allowed  $1\text{-}\sigma$  and  $2\text{-}\sigma$  regions in the  $m_\phi$ - $g_\phi$  plane from IceCube data are shown along with the bounds from the cosmological bound (“Planck+BAO+HST”) for  $\nu_\tau$ - $\nu_\tau$  interaction in the normal hierarchy. The allowed region for IceCube has no overlap with the strong self-interaction (SI) band.

flux of the neutrinos by the maximum allowed values of all the parameters ( $m_\phi, g_\phi, \gamma$  and  $m_0$ ) within the  $1\text{-}\sigma$  range. The shaded region shows that the dip in the specific flux can reach only up to a certain minima and it cannot go deeper since that will require larger neutrino masses than the specified upper bound on  $m_0$  in table 3. We have also plotted a red solid line and a dashed orange line of the specific flux. The red solid line corresponds to bestfit values of all the parameters. Whereas, the orange line corresponds to the  $m_0 = 0$  eV and all other parameters  $m_\phi, g_\phi$  and  $\gamma$  fixed to their best-fit values. As discussed in the previous section, “Planck+BAO+HST” data also puts a bound on  $G_{\text{eff}}$ , which translate into a bound on  $m_\phi$ - $g_\phi$  parameter space. The  $1\text{-}\sigma$  and  $2\text{-}\sigma$  bounds for both SI and MI region have been shown by the green and gray shaded area respectively in fig. (5)-(b). It is quite evident from fig. (5)-(b) that the IceCube allowed parameter space for  $m_\phi$ - $g_\phi$  is inconsistent with SI bound. Whereas, some part of IceCube allowed parameter space for  $m_\phi$ - $g_\phi$  overlaps with MI bound at  $2\text{-}\sigma$  level only.

**$\nu_\tau$ - $\nu_\tau$  interactions:** The main difference in the features of flavour specific interaction and universal interaction is that while flavour specific interaction can produce two prominent dips in two different energy bins of IceCube data, the universal interaction allows only one prominent dip. However, the two dips in a flavour specific interaction can be merged to one by increasing the neutrino mass. The bestfit values along with  $1\text{-}\sigma$  error for all the parameters ( $m_\phi, g_\phi, \gamma$  and  $m_0$ ) is given in table 3. The specific flux of the neutrinos corresponds to the  $1\text{-}\sigma$  allowed values of all these parameters is shown by the shaded region in the fig. (6)-(a). We have also plotted two different lines, the solid red and orange dashed line, for specific flux in IceCube which show quite different features. For the orange dashed line,  $m_0$  has been taken to be zero and all other parameters has been kept at their best fit values. This line can explain two dips in IceCube data at two different energies. If the neutrino mass is increased, the orange dashed line in the figure moves towards the solid red line which corresponds to the



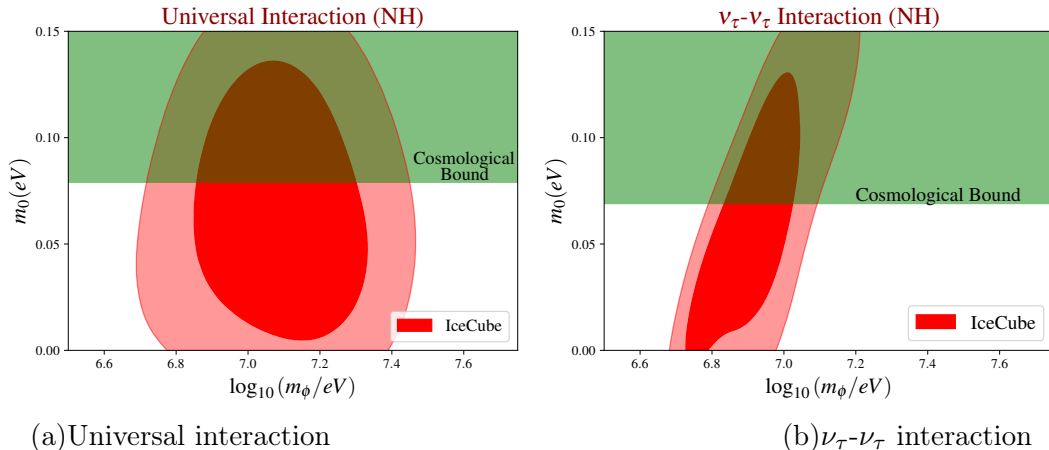


**Figure 7:** The green region shows the values of lowest neutrino mass ( $m_0$ ) excluded by cosmological data (“Planck+BAO+HST”) for the normal hierarchy. A major portion of the preferred  $m_0$  values by IceCube data is disfavored by the cosmological bound.

Parameter	68% limits
<b>Universal interaction</b>	
$m_0$ (eV)	$0.067^{+0.038}_{-0.046}$
$\log_{10}(m_\phi/\text{eV})$	$7.09 \pm 0.15$
$\log_{10} g_\phi$	$-1.75 \pm 0.31$
$\gamma$	$2.66^{+0.21}_{-0.18}$
<b><math>\nu_\tau</math>-<math>\nu_\tau</math> interaction</b>	
$m_0$ (eV)	$0.062^{+0.042}_{-0.046}$
$\log_{10} m_\phi/\text{eV}$	$6.92 \pm 0.11$
$\log_{10} g_\phi$	$-1.40 \pm 0.13$
$\gamma$	$2.50 \pm 0.17$

**Table 3:** The preferred bestfit values of the IceCube parameters and their 1- $\sigma$  ranges for both universal and  $\nu_\tau$ - $\nu_\tau$  interaction case in the **normal hierarchy**. are listed in this table

bestfit values of all the parameters presented in table 3. Therefore we see in the fig. (6)-(a) that the solid red line and the orange dashed line represent the one and two dip solutions in the IceCube energy range. Similar to the universal case, it is quite evident from fig. (6)-(b) that the IceCube allowed parameter space for  $m_\phi$ - $g_\phi$  is inconsistent with SI region. Whereas, IceCube allowed parameter space for  $m_\phi$ - $g_\phi$  is consistent with MI bound at 2- $\sigma$  level. We have also presented the IceCube allowed parameter space for  $m_\phi$ - $m_0$  in fig. (7)-(b). The cosmological 1- $\sigma$  upper bound of  $m_0$  is 0.069 eV for moderate  $\nu_\tau$ - $\nu_\tau$  interaction in case of normal hierarchy. The disallowed region is shown in the green color in fig. (7)-(b), which rules out a substantial part of IceCube allowed  $m_0$  values.

## 5.2 Inverted Hierarchy

**Universal interactions:** Similar to the case of normal hierarchy, in the case of inverted hierarchy, the universal interaction produces a flatter specific flux line compared to the flavour specific interactions for smaller values of  $m_0$  as well. Since large values of  $m_0$  make masses

of different neutrino mass eigenstates almost degenerate, we get a single dip solution for such case. Therefore, again to fit the dips in the IceCube data the universal interaction prefers a higher value of  $m_0$ . The bestfit values along with 1- $\sigma$  error for all the parameters ( $m_\phi, g_\phi, \gamma$  and  $m_0$ ) are given in table 4. "Planck+BAO+HST" data also put a bound on the lowest neutrino mass  $m_0 \leq 0.083$  eV for the moderate universal interaction in the inverted hierarchy. The values of  $m_0$  excluded by the cosmological data are shown in the green shaded region in fig. (10), which clearly implies that a substantial fraction of the IceCube preferred mass range is disallowed by the cosmological bound.

In fig. (8), the specific flux in IceCube and the corresponding allowed parameter space for  $m_\phi$ - $g_\phi$  have been shown. The shaded region in the fig. (8)-(a) corresponds to the specific flux of the neutrinos for the maximum allowed values of all the parameters ( $m_\phi, g_\phi, \gamma$  and  $m_0$ ) within the 1- $\sigma$  range. Similar to the normal hierarchy case, the shaded region shows that the dip in the specific flux can reach only up to a certain minima and it cannot go deeper cause that will require larger neutrino masses. We have also plotted a red solid line and a dashed orange line of specific flux. The red solid line corresponds to the best fit values of all the parameters listed in table 4. Whereas, the orange line corresponds to the  $m_0 = 0$  eV and all other parameters fixed at their best fit values. Similar to the normal hierarchy, It is quite evident from fig. (8)-(b) that the IceCube allowed parameter space for  $m_\phi$ - $g_\phi$  is inconsistent with SI bound. However, some part of IceCube allowed parameter space for  $m_\phi$ - $g_\phi$  overlaps with MI bound at 2- $\sigma$  level only.

**$\nu_\tau$ - $\nu_\tau$  interactions:** In case of inverted hierarchy, for the  $\nu_\tau$ - $\nu_\tau$  interaction, number of dips in the IceCube energy range depends on the  $m_0$  value. For very small value of  $m_0$  (close to zero) we get one dip in the IceCube energy range. Similarly, in the case of larger values of  $m_0$ , when all the three mass eigenstates become almost degenerate, we find only one dip in the IceCube energy range. On the other hand, for the values of  $m_0$ , which are not very close to zero and also not very large to make all three mass eigenstates degenerate, we can get two dips in the IceCube energy range. The bestfit values along with 1- $\sigma$  error for all the parameters ( $m_\phi, g_\phi, \gamma$  and  $m_0$ ) are given in table 4. In fig. (9), the specific flux in IceCube and the corresponding allowed parameter space for  $m_\phi$ - $g_\phi$  have been shown. We have also plotted three different lines, the solid red, orange dashed and dotted pink line, for the specific flux in IceCube which show very different features. The orange dashed line is for  $m_0 = 0$  eV and all

Parameter	68% limits
<b><u>Universal interaction</u></b>	
$m_0$ (eV)	$0.052^{+0.034}_{-0.040}$
$\log_{10}(m_\phi/\text{eV})$	$6.883 \pm 0.091$
$\log_{10} g_\phi$	$-1.87 \pm 0.20$
$\gamma$	$2.63 \pm 0.17$
<b><u><math>\nu_\tau</math>-<math>\nu_\tau</math> interaction</u></b>	
$m_0$ (eV)	$0.062^{+0.038}_{-0.058}$
$\log_{10}(m_\phi/\text{eV})$	$6.936^{+0.089}_{-0.14}$
$\log_{10} g_\phi$	$-1.25 \pm 0.17$
$\gamma$	$2.46^{+0.18}_{-0.16}$

**Table 4:** The preferred bestfit values of the IceCube parameters and their 1- $\sigma$  ranges for both universal and  $\nu_\tau$ - $\nu_\tau$  interaction case in the **inverted hierarchy**. are listed in this table.

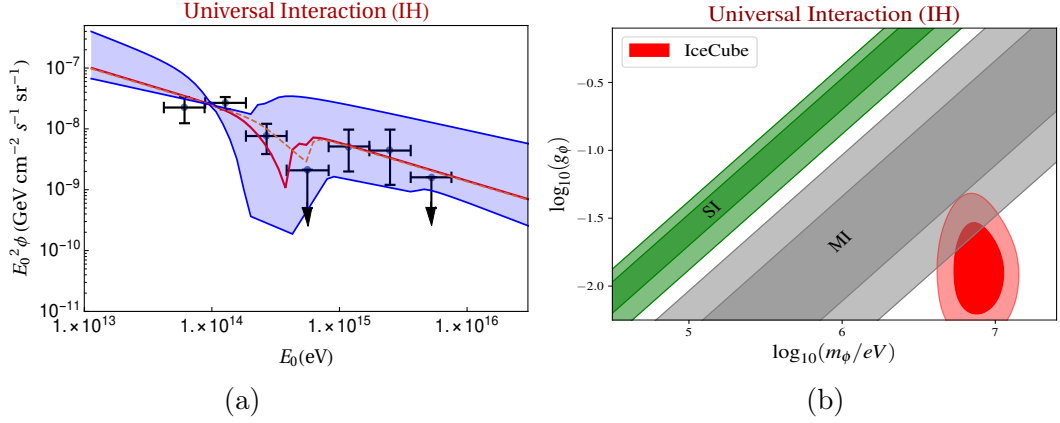


**Figure 8: Universal interaction in inverted hierarchy:** (a) The shaded region corresponds to the specific flux of the neutrinos allowed by the  $1\text{-}\sigma$  ranges of the parameters in table 4. The solid red line correspond to the best fit values of the parameters and the orange dashed line corresponds to the best fit value of  $m_\phi, g_\phi$  and  $\gamma$  (in table 4) and the value of  $m_0$  is fixed at zero. (b) The allowed  $1\text{-}\sigma$  and  $2\text{-}\sigma$  regions in the  $m_\phi\text{-}g_\phi$  plane from IceCube data are shown along with the cosmological bound (“Planck+BAO+HST”) for universal interaction in the inverted hierarchy. The allowed region for IceCube has no overlap with the strong self-interaction (SI) band.

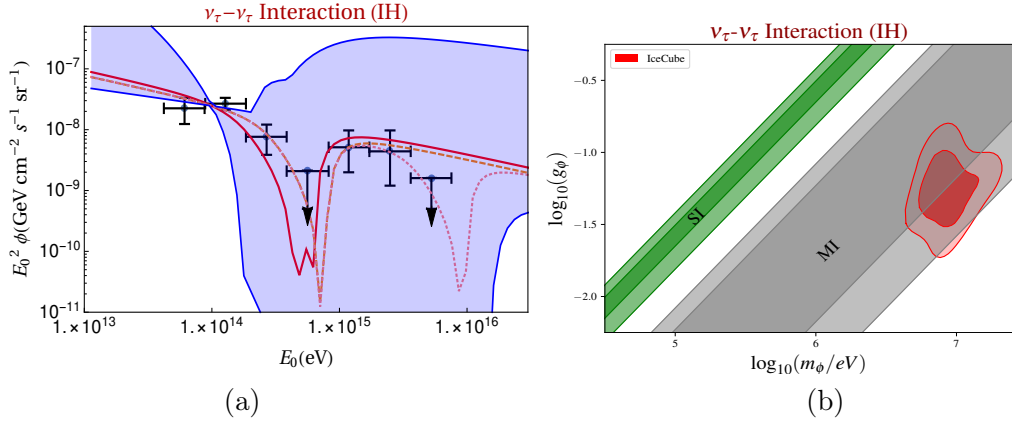


**Figure 9:  $\nu_\tau\text{-}\nu_\tau$  interaction in inverted hierarchy:** (a) The shaded region corresponds to the specific flux of the neutrinos allowed by the  $1\text{-}\sigma$  ranges of all the parameters in table 4. The values of  $m_\phi, g_\phi$  and  $\gamma$  has been fixed to their bestfit values (in table 4) for all the solid red line, orange dashed line and the pink dotted line. However, the solid red line corresponds to the bestfit value of  $m_0$ ; the orange dashed line corresponds to the  $m_0$  value fixed at zero and the pink dotted line corresponds to the lowest  $1\text{-}\sigma$  allowed value of  $m_0$ . (b) The allowed  $1\text{-}\sigma$  and  $2\text{-}\sigma$  regions in the  $m_\phi\text{-}g_\phi$  plane from IceCube data are shown along with the cosmological bound (“Planck+BAO+HST”) for  $\nu_\tau\text{-}\nu_\tau$  interaction in the inverted hierarchy. The allowed region for IceCube has no overlap with the strong self-interaction (SI) band.

other parameters are fixed at their best fit values. We can see from the fig. (9)-(a) that this line represents the one dip solution. As we increase the  $m_0$  value, the orange dashed line moves towards the pink dotted line. In case of the pink dotted line, we have kept the value of  $m_0$  fixed

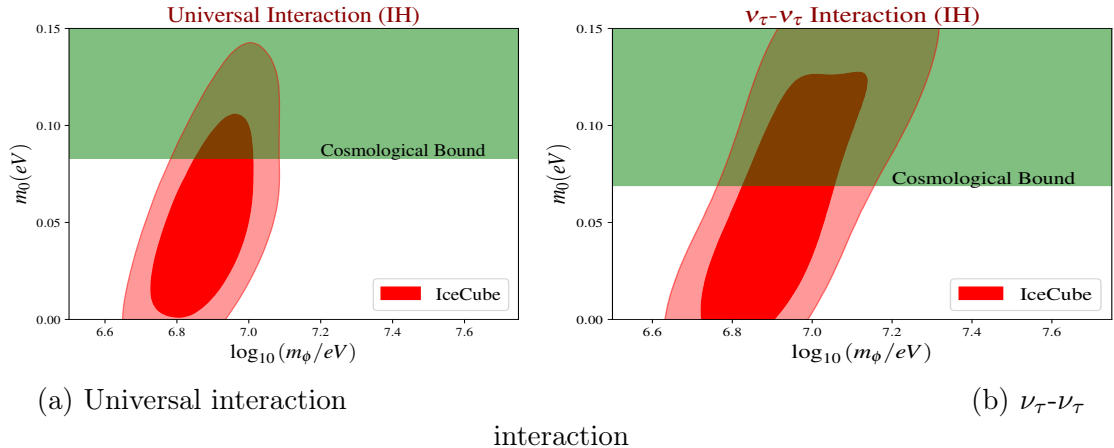


**Figure 10:** The green region shows the values of lowest neutrino mass ( $m_0$ ) excluded by cosmological data (“Planck+BAO+HST”) for the inverted hierarchy. For both the interaction cases, a significant portion of the preferred  $m_0$  values by IceCube data is excluded by the cosmological bound.

at lowest 1- $\sigma$  value. It can be clearly seen from the fig. (9)-(a) that pink dotted line can explain two dips in IceCube data at two different energies. If the neutrino mass is increased further the pink dotted line moves towards the solid red line which corresponds to the bestfit values of the all parameters presented in table 4. Therefore, we can clearly see from the fig. (9)-(a) that the solid red and orange dashed line represent the one dip solutions in the IceCube energy range, whereas the pink dotted line represents the two dip solution. The shaded region in the fig. (9)-(a) corresponds to the specific flux of the neutrinos for the maximum allowed values of all the parameters ( $m_\phi, g_\phi, \gamma$  and  $m_0$ ) within the 1- $\sigma$ . Once again, It is quite evident from fig. (9)-(b) that the IceCube allowed parameter space for  $m_\phi$ - $g_\phi$  is inconsistent with SI bound. However, IceCube allowed parameter space for  $m_\phi$ - $g_\phi$  is consistent with MI bound at 1- $\sigma$  level. We have also presented the IceCube allowed parameter space for  $m_\phi$ - $m_0$  in fig. (10)-(b). The 1- $\sigma$  maximum value of  $m_0$  allowed by “Planck+BAO+HST” data is 0.069 eV for moderate  $\nu_\tau$ - $\nu_\tau$  interaction in case of inverted hierarchy. This cosmological disallowed region is shown in the green shade in fig. (7)-(b) which implies that a substantial part of IceCube allowed  $m_0$  values is ruled out by the cosmological bound.

## 6 Conclusions

In this paper we have studied the self-interaction between the neutrinos in the context of  $H_0$  tension and the observed dips in the neutrino flux at IceCube . We have shown that the flavour specific interaction and the universal interaction does not affect CMB power spectrum very much differently. Even the inverted hierarchy and the normal hierarchy do not have much distinguishable effect. The bound on the self interaction parameter  $G_{\text{eff}}$  from the “Planck+BAO+HST” data shows a bimodal feature in its distribution which is consistent with the earlier studies. The bestfit values of  $G_{\text{eff}}$  from the MCMC analysis are also similar for different types of interaction in different hierarchies. If self-interaction is not considered in the neutrinos, the allowed value of  $N_{\text{eff}}$  predicts  $H_0$  much lower than the value obtained from HST measurement [18]. Whereas, for the cosmological model having self-interacting neutrinos, the  $H_0$  value obtained in a joint analysis of Planck CMB, BAO, and HST data is

higher than that obtained from the  $\Lambda$ CDM model. In that case, the obtained  $H_0$  overlaps with the  $H_0$  from the HST measurement. However, it should be noted that for the self-interacting neutrino model, the  $H_0$  inferred from the Planck CMB data alone does not change much from the  $H_0$  values obtained within the  $\Lambda$ CDM model.

The effect of the flavour specific and the universal interaction on the total flux of astrophysical neutrinos in IceCube is quite different. We have plotted different ways of fitting IceCube data with these interactions and constrained the parameter space of self-interaction mediator and the neutrino mass. We find that the dips in between 400 TeV -1 PeV and at around 6 PeV can be simultaneously explained using the neutrino self-interaction in flavour specific cases<sup>3</sup>. However, in case of universal interaction it is impossible to explain two dips simultaneously and by adjusting the parameters, only one dip can be explained. Moreover, by suitably adjusting the lowest neutrino mass, two different dips in flavour specific cases can also be merged into a single dip. We find that there is no distinguishable difference in the features of the neutrino flux line for  $\nu_e$ - $\nu_e$ ,  $\nu_\mu$ - $\nu_\mu$  and  $\nu_\tau$ - $\nu_\tau$  interaction. Therefore, all the analysis and the results presented here for the  $\nu_\tau$ - $\nu_\tau$  interaction are equally applicable to the  $\nu_e$ - $\nu_e$  and  $\nu_\mu$ - $\nu_\mu$  interaction cases.

Hierarchies also play an important role in determining the position and the shape of the absorption dips in the neutrino flux at IceCube. In the case of universal interaction and normal hierarchy, two very small dips can occur for the lowest neutrino mass being zero. However, for the same case in the inverted hierarchy, there can be only one small dip if  $m_0$  is fixed at zero. In case of  $\nu_\tau$ - $\nu_\tau$  interaction, normal hierarchy can produce two dips in the two above-mentioned energy values (around 500 TeV and 6 PeV) for the value of  $m_0$  fixed at zero. However, in the case of inverted hierarchy, that same feature requires a small but non-zero lowest neutrino mass.

Since, the value of mediator mass ( $m_\phi$ ) changes the position of the dips and the value of the interaction strength ( $g_\phi$ ) changes the sharpness of the dips, the MCMC analysis provide quite strict bound on those values. Larger values of  $g_\phi$  beyond the obtained bound can produce sharper dips in the resonance energies, but it will not be able to explain the absorption feature throughout the specified energy range of a certain bin in the IceCube data. We found that the cosmological bound on the neutrino self-interaction parameters in strong interaction (SI) region, which are inferred from the joint analysis of Planck, HST and BAO data, are inconsistent with the parameter space inferred from the IceCube data. The preferred parameter space of  $g_\phi$ - $m_\phi$  by the IceCube data can only be slightly consistent with the moderate interaction (MI) allowed by the cosmological data set. More specifically, only the  $\nu_\tau$ - $\nu_\tau$  interaction in the inverted hierarchy prefers  $g_\phi$ - $m_\phi$  parameter space that is in 1- $\sigma$  concordance with cosmological constraints. For all other cases of neutrino self-interactions studied in this paper allowed parameter space from IceCube data and cosmological data matches at 2- $\sigma$  level only. We have also plotted the allowed region of flux line beyond 10 PeV neutrino energy in our results. Therefore, it serves as a prediction for upcoming data in IceCube experiment in ultra high energies.

---

<sup>3</sup>The recent observation [31] of the Glashow resonance event by the IceCube collaboration might impact this conclusion. However, we expect the change in constrained parameter space will not affect the paper's conclusion. This is because of the observed flux at around 6 PeV in ref. [31] overlaps significantly with the 1- $\sigma$  band shown in our plots (fig. (5)-a, fig. (6)-a, fig. (8)-a, and fig. (9)-a)

## Acknowledgment

We acknowledge the computation facility, 100TFLOP HPC Cluster, Vikram-100, at Physical Research Laboratory, Ahmedabad, India. The authors sincerely thank the referee for their insightful comments and suggestions that helped in improving the structure and quality of this paper. Some part of this manuscript during the last stage of the review was completed during PP's tenure at Indian Institute of science for which PP acknowledge IOE-IISc fellowship program for financial assistance.

## Appendix

### A Numerical details

The MCMC analysis performed in the paper for the IceCube data is based upon the Metropolis-Hastings algorithm [76]. The likelihood function used in the analysis assumes a generalized likelihood function for asymmetric error, following ref. [77] which can be written as

$$\ln[L] = \sum -\frac{1}{2} \left( \frac{\hat{x} - x}{\sigma + \sigma'(\hat{x} - x)} \right)^2, \quad (\text{A.1})$$

where,

$$\sigma = \frac{2\sigma_+\sigma_-}{\sigma_+ + \sigma_-} \text{ and } \sigma' = \frac{\sigma_+ - \sigma_-}{\sigma_+ + \sigma_-}, \quad (\text{A.2})$$

with  $\sigma_+$  and  $\sigma_-$  are the positive and negative errors. In case of symmetric errors  $\ln[L]$  turns out to be  $-\chi^2$ . In the likelihood function we used the binned flux data of ref. [75] as observational values. Theoretical values are calculated from the solution of eq. (4.5) for 63 different points in the IceCube energy range where we have taken 9 points from each bin in equally spaced log space of  $E_0$ .

We have used the Gaussian priors for all the parameters and the corresponding values are given table 5. We have also set the maximum and minimum values at 7.4 and 6.2 respectively for  $\log_{10}(m_\phi/\text{eV})$ . Lowest neutrino mass  $m_0$  has also been assigned with maximum and minimum values of 0.15 eV and 0 respectively.

The cosmological parameters of interest in this paper are the six standard cosmological parameters, effective number of relativistic degrees of freedom  $N_{\text{eff}}$ , lowest neutrino mass  $m_0$  and effective coupling constant of self-interaction ( $G_{\text{eff}}$ ). The six standard cosmological parameters are: the fraction density of cold dark matter and baryonic matter at present multiplied by square of the reduced Hubble parameter ( $\omega_{\text{cdm}}$  and  $\omega_b$  respectively), acoustic scale of baryon acoustic oscillation ( $\theta_s$ ), amplitude and the spectral index of the primordial

Parameter	mean	1- $\sigma$
$m_0(\text{eV})$	0.05	0.02
$\log_{10}(m_\phi/\text{eV})$	6.7	0.05
$\log_{10} g_\phi$	-1.5	0.05
$\gamma$	2.35	0.05

**Table 5:** Priors used in MCMC with IceCube data

density perturbations ( $A_s$  and  $n_s$  respectively) and optical depth to the epoch of re-ionization ( $\tau_{\text{reion}}$ ). These nine parameters have been varied in this analysis and the corresponding priors for these parameters are given in table 6. We have used Gaussian prior for our purpose.

Parameter	mean	1- $\sigma$
$\omega_b$	$2.2377 \times 10^{-2}$	$0.015 \times 10^{-2}$
$\omega_{\text{cdm}}$	0.12010	0.0013
$100\theta_s$	1.04110	3e-4
$\ln(10^{10}A_s)$	3.0447	0.015
$n_s$	0.9659	0.0042
$\tau_{\text{reio}}$	0.0543	0.008
$\log_{10}(G_{\text{eff}})$	-1.5	0.2
$m_0$	0.008	0.005
$N_{\text{eff}}$	3.75	0.1

**Table 6:** Priors used in MCMC with Planck, BAO and HST data.

In case of  $\log_{10}(G_{\text{eff}})$ , we have assigned the maximum and minimum values -5.0 and -0.1 respectively. Lowest neutrino mass  $m_0$  has been varied in the range [0, 0.2] eV and  $N_{\text{eff}}$  has been varied in the range [3,5]. We have also assigned a minimum value of  $\tau_{\text{reio}}$  at 0.04. While sampling the parameter space, we increased temperature of the chains by a factor of three following ref [2] for proper sampling.

To show the comparison between different models under consideration in this work, we report the maximum value of likelihood (minimum of  $-\log(\text{likelihood})$ ) in Table 7. It is evident from this table that there is a significant improvement in the  $-\log(\text{likelihood})$  values after the inclusion of self-interaction in neutrinos for the joint analysis of Planck, BAO, and HST data.

Model	$-\log(\text{likelihood})$
$\Lambda\text{CDM}$	794.84
Universal Interaction (NH)	263.89
Universal Interaction (IH)	263.51
$\nu_\tau$ - $\nu_\tau$ Interaction (NH)	264.02
$\nu_\tau$ - $\nu_\tau$ Interaction (IH)	236.58

**Table 7:** The  $-\log(\text{likelihood})$  values obtained from the MCMC analysis of the cosmological model with universal and  $\nu_\tau$ - $\nu_\tau$  self interactions and the standard  $\Lambda\text{CDM}$  model.

## References

- [1] L. Lancaster, F.-Y. Cyr-Racine, L. Knox, and Z. Pan, *A tale of two modes: Neutrino free-streaming in the early universe*, *JCAP* **07** (2017) 033, [[arXiv:1704.06657](#)].
- [2] I. M. Oldengott, T. Tram, C. Rampf, and Y. Y. Wong, *Interacting neutrinos in cosmology: exact description and constraints*, *JCAP* **11** (2017) 027, [[arXiv:1706.02123](#)].
- [3] C. D. Kreisch, F.-Y. Cyr-Racine, and O. Doré, *Neutrino puzzle: Anomalies, interactions, and cosmological tensions*, *Phys. Rev. D* **101** (2020), no. 12 123505, [[arXiv:1902.00534](#)].



- [4] M. Park, C. D. Kreisch, J. Dunkley, B. Hadzhiyska, and F.-Y. Cyr-Racine,  *$\Lambda$ CDM or self-interacting neutrinos: How CMB data can tell the two models apart*, *Phys. Rev. D* **100** (2019), no. 6 063524, [[arXiv:1904.02625](#)].
- [5] G. Barenboim, P. B. Denton, and I. M. Oldengott, *Constraints on inflation with an extended neutrino sector*, *Phys. Rev. D* **99** (2019), no. 8 083515, [[arXiv:1903.02036](#)].
- [6] A. Mazumdar, S. Mohanty, and P. Parashari, *Inflation models in the light of self-interacting sterile neutrinos*, *Phys. Rev. D* **101** (2020), no. 8 083521, [[arXiv:1911.08512](#)].
- [7] N. Blinov and G. Marques-Tavares, *Interacting radiation after Planck and its implications for the Hubble Tension*, *JCAP* **09** (2020) 029, [[arXiv:2003.08387](#)].
- [8] H.-J. He, Y.-Z. Ma, and J. Zheng, *Resolving Hubble Tension by Self-Interacting Neutrinos with Dirac Seesaw*, *JCAP* **11** (2020) 003, [[arXiv:2003.12057](#)].
- [9] A. Das, A. Dighe, and M. Sen, *New effects of non-standard self-interactions of neutrinos in a supernova*, *JCAP* **05** (2017) 051, [[arXiv:1705.00468](#)].
- [10] H. Ko et al., *Neutrino Process in Core-collapse Supernovae with Neutrino Self-interaction and MSW Effects*, *Astrophys. J. Lett.* **891** (2020), no. 1 L24.
- [11] K. Blum, A. Hook, and K. Murase, *High energy neutrino telescopes as a probe of the neutrino mass mechanism*, [[arXiv:1408.3799](#)].
- [12] N. Blinov, K. J. Kelly, G. Z. Krnjaic, and S. D. McDermott, *Constraining the Self-Interacting Neutrino Interpretation of the Hubble Tension*, *Phys. Rev. Lett.* **123** (2019), no. 19 191102, [[arXiv:1905.02727](#)].
- [13] V. Brdar, M. Lindner, S. Vogl, and X.-J. Xu, *Revisiting neutrino self-interaction constraints from  $Z$  and  $\tau$  decays*, *Phys. Rev. D* **101** (2020), no. 11 115001, [[arXiv:2003.05339](#)].
- [14] K. C. Y. Ng and J. F. Beacom, *Cosmic neutrino cascades from secret neutrino interactions*, *Phys. Rev. D* **90** (2014), no. 6 065035, [[arXiv:1404.2288](#)]. [Erratum: *Phys.Rev.D* 90, 089904 (2014)].
- [15] A. DiFranzo and D. Hooper, *Searching for MeV-Scale Gauge Bosons with IceCube*, *Phys. Rev. D* **92** (2015), no. 9 095007, [[arXiv:1507.03015](#)].
- [16] I. M. Shoemaker and K. Murase, *Probing BSM Neutrino Physics with Flavor and Spectral Distortions: Prospects for Future High-Energy Neutrino Telescopes*, *Phys. Rev. D* **93** (2016), no. 8 085004, [[arXiv:1512.07228](#)].
- [17] M. Bustamante, C. Rosenstrøm, S. Shalgar, and I. Tamborra, *Bounds on secret neutrino interactions from high-energy astrophysical neutrinos*, *Phys. Rev. D* **101** (2020), no. 12 123024, [[arXiv:2001.04994](#)].
- [18] **Planck** Collaboration, N. Aghanim et al., *Planck 2018 results. VI. Cosmological parameters*, [[arXiv:1807.06209](#)].
- [19] G. Efstathiou,  *$H_0$  Revisited*, *Mon. Not. Roy. Astron. Soc.* **440** (2014), no. 2 1138–1152, [[arXiv:1311.3461](#)].
- [20] J. L. Bernal, L. Verde, and A. G. Riess, *The trouble with  $H_0$* , *JCAP* **10** (2016) 019, [[arXiv:1607.05617](#)].
- [21] L. Verde, T. Treu, and A. Riess, *Tensions between the early and late universe*, *Nature Astronomy* **03** (Sep, 2019) 891–895, [[arXiv:1907.10625](#)].
- [22] E. Di Valentino et al., *Cosmology Intertwined II: The Hubble Constant Tension*, [[arXiv:2008.11284](#)].
- [23] A. G. Riess, S. Casertano, W. Yuan, L. M. Macri, and D. Scolnic, *Large Magellanic Cloud Cepheid Standards Provide a 1% Foundation for the Determination of the Hubble Constant and*

- Stronger Evidence for Physics beyond  $\Lambda$ CDM*, *Astrophys. J.* **876** (2019), no. 1 85, [[arXiv:1903.07603](#)].
- [24] K.-F. Lyu, E. Stamou, and L.-T. Wang, *Self-interacting neutrinos: solution to Hubble tension versus experimental constraints*, [arXiv:2004.10868](#).
- [25] F. F. Deppisch, L. Graf, W. Rodejohann, and X.-J. Xu, *Neutrino Self-Interactions and Double Beta Decay*, *Phys. Rev. D* **102** (2020), no. 5 051701, [[arXiv:2004.11919](#)].
- [26] K. Ioka and K. Murase, *IceCube PeV–EeV neutrinos and secret interactions of neutrinos*, *PTEP* **2014** (2014), no. 6 061E01, [[arXiv:1404.2279](#)].
- [27] B. Chauhan and S. Mohanty, *Signature of light sterile neutrinos at IceCube*, *Phys. Rev. D* **98** (2018), no. 8 083021, [[arXiv:1808.04774](#)].
- [28] K. J. Kelly and P. A. Machado, *Multimessenger Astronomy and New Neutrino Physics*, *JCAP* **10** (2018) 048, [[arXiv:1808.02889](#)].
- [29] S. Mohanty, A. Narang, and S. Sadhukhan, *Cutoff of IceCube Neutrino Spectrum due to  $t$ -channel Resonant Absorption by  $C\nu B$* , *JCAP* **03** (2019) 041, [[arXiv:1808.01272](#)].
- [30] C. Creque-Sarbinowski, J. Hyde, and M. Kamionkowski, *Resonant Neutrino Self-Interactions*, [arXiv:2005.05332](#).
- [31] **IceCube** Collaboration, M. G. Aartsen et al., *Detection of a particle shower at the Glashow resonance with IceCube*, *Nature* **591** (2021), no. 7849 220–224, [[arXiv:2110.15051](#)]. [Erratum: *Nature* 592, E11 (2021)].
- [32] Y. Chikashige, R. N. Mohapatra, and R. Peccei, *Are There Real Goldstone Bosons Associated with Broken Lepton Number?*, *Phys. Lett. B* **98** (1981) 265–268.
- [33] G. Gelmini and M. Roncadelli, *Left-Handed Neutrino Mass Scale and Spontaneously Broken Lepton Number*, *Phys. Lett. B* **99** (1981) 411–415.
- [34] H. M. Georgi, S. L. Glashow, and S. Nussinov, *Unconventional Model of Neutrino Masses*, *Nucl. Phys. B* **193** (1981) 297–316.
- [35] G. B. Gelmini, S. Nussinov, and M. Roncadelli, *Bounds and Prospects for the Majoron Model of Left-handed Neutrino Masses*, *Nucl. Phys. B* **209** (1982) 157–173.
- [36] S. Nussinov and M. Roncadelli, *Observable Effects of Relic Majorons*, *Phys. Lett. B* **122** (1983) 387–391.
- [37] U. K. Dey, N. Nath, and S. Sadhukhan, *Charged Higgs effects in IceCube: PeV events and NSIs*, [arXiv:2010.05797](#).
- [38] F. Arias-Aragon, E. Fernandez-Martinez, M. Gonzalez-Lopez, and L. Merlo, *Neutrino Masses and Hubble Tension via a Majoron in MFV*, [arXiv:2009.01848](#).
- [39] M. Berbig, S. Jana, and A. Trautner, *The Hubble tension and a renormalizable model of gauged neutrino self-interactions*, [arXiv:2004.13039](#).
- [40] I. Esteban, M. Gonzalez-Garcia, M. Maltoni, T. Schwetz, and A. Zhou, *The fate of hints: updated global analysis of three-flavor neutrino oscillations*, [arXiv:2007.14792](#).
- [41] H. Goldberg, G. Perez, and I. Sarcevic, *Mini  $Z'$  burst from relic supernova neutrinos and late neutrino masses*, *JHEP* **11** (2006) 023, [[hep-ph/0505221](#)].
- [42] Y. Farzan and S. Palomares-Ruiz, *Dips in the Diffuse Supernova Neutrino Background*, *JCAP* **06** (2014) 014, [[arXiv:1401.7019](#)].
- [43] C.-P. Ma and E. Bertschinger, *Cosmological perturbation theory in the synchronous and conformal Newtonian gauges*, *Astrophys. J.* **455** (1995) 7–25, [[astro-ph/9506072](#)].
- [44] I. M. Oldengott, C. Rampf, and Y. Y. Y. Wong, *Boltzmann hierarchy for interacting neutrinos I: formalism*, *JCAP* **04** (2015) 016, [[arXiv:1409.1577](#)].

- [45] M. Archidiacono, E. Calabrese, and A. Melchiorri, *The Case for Dark Radiation*, *Phys. Rev. D* **84** (2011) 123008, [[arXiv:1109.2767](#)].
- [46] T. L. Smith, S. Das, and O. Zahn, *Constraints on neutrino and dark radiation interactions using cosmological observations*, *Phys. Rev. D* **85** (2012) 023001, [[arXiv:1105.3246](#)].
- [47] N. Song, M. Gonzalez-Garcia, and J. Salvado, *Cosmological constraints with self-interacting sterile neutrinos*, *JCAP* **10** (2018) 055, [[arXiv:1805.08218](#)].
- [48] S. Hannestad and R. J. Scherrer, *Selfinteracting warm dark matter*, *Phys. Rev.* **D62** (2000) 043522, [[astro-ph/0003046](#)].
- [49] A. Das and S. Ghosh, *Flavor-specific Interaction Favours Strong Neutrino Self-coupling*, [[arXiv:2011.12315](#)].
- [50] F. Forastieri, M. Lattanzi, G. Mangano, A. Mirizzi, P. Natoli, and N. Saviano, *Cosmic microwave background constraints on secret interactions among sterile neutrinos*, *JCAP* **07** (2017) 038, [[arXiv:1704.00626](#)].
- [51] J. Lesgourgues, *The Cosmic Linear Anisotropy Solving System (CLASS) I: Overview*, [[arXiv:1104.2932](#)].
- [52] B. Audren, J. Lesgourgues, K. Benabed, and S. Prunet, *Conservative Constraints on Early Cosmology: an illustration of the Monte Python cosmological parameter inference code*, *JCAP* **1302** (2013) 001, [[arXiv:1210.7183](#)].
- [53] **Planck** Collaboration, Y. Akrami et al., *Planck 2018 results. X. Constraints on inflation*, [[arXiv:1807.06211](#)].
- [54] **BOSS** Collaboration, S. Alam et al., *The clustering of galaxies in the completed SDSS-III Baryon Oscillation Spectroscopic Survey: cosmological analysis of the DR12 galaxy sample*, *Mon. Not. Roy. Astron. Soc.* **470** (2017), no. 3 2617–2652, [[arXiv:1607.03155](#)].
- [55] A. Lewis, *GetDist: a Python package for analysing Monte Carlo samples*, [[arXiv:1910.13970](#)].
- [56] M. Ahlers, L. A. Anchordoqui, and S. Sarkar, *Neutrino diagnostics of ultra-high energy cosmic ray protons*, *Phys. Rev. D* **79** (2009) 083009, [[arXiv:0902.3993](#)].
- [57] **IceCube** Collaboration, M. G. Aartsen et al., *The contribution of Fermi-2LAC blazars to the diffuse TeV-PeV neutrino flux*, *Astrophys. J.* **835** (2017), no. 1 45, [[arXiv:1611.03874](#)].
- [58] D. Hooper, T. Linden, and A. Vieregg, *Active Galactic Nuclei and the Origin of IceCube’s Diffuse Neutrino Flux*, *JCAP* **02** (2019) 012, [[arXiv:1810.02823](#)].
- [59] C. Yuan, K. Murase, and P. Mészáros, *Complementarity of Stacking and Multiplet Constraints on the Blazar Contribution to the Cumulative High-Energy Neutrino Intensity*, *Astrophys. J.* **890** (2020) 25, [[arXiv:1904.06371](#)].
- [60] J.-W. Luo and B. Zhang, *Blazar - IceCube neutrino association revisited*, *Phys. Rev. D* **101** (2020), no. 10 103015, [[arXiv:2004.09686](#)].
- [61] D. Smith, D. Hooper, and A. Vieregg, *Revisiting AGN as the source of IceCube’s diffuse neutrino flux*, *JCAP* **03** (2021) 031, [[arXiv:2007.12706](#)].
- [62] E. Waxman and J. N. Bahcall, *High-energy neutrinos from cosmological gamma-ray burst fireballs*, *Phys. Rev. Lett.* **78** (1997) 2292–2295, [[astro-ph/9701231](#)].
- [63] **IceCube** Collaboration, R. Abbasi et al., *Search for muon neutrinos from Gamma-Ray Bursts with the IceCube neutrino telescope*, *Astrophys. J.* **710** (2010) 346–359, [[arXiv:0907.2227](#)].
- [64] **IceCube** Collaboration, R. Abbasi et al., *Limits on Neutrino Emission from Gamma-Ray Bursts with the 40 String IceCube Detector*, *Phys. Rev. Lett.* **106** (2011) 141101, [[arXiv:1101.1448](#)].

- [65] **IceCube** Collaboration, R. Abbasi et al., *An absence of neutrinos associated with cosmic-ray acceleration in  $\gamma$ -ray bursts*, *Nature* **484** (2012) 351–353, [[arXiv:1204.4219](#)].
- [66] **IceCube** Collaboration, M. G. Aartsen et al., *Search for Prompt Neutrino Emission from Gamma-Ray Bursts with IceCube*, *Astrophys. J. Lett.* **805** (2015), no. 1 L5, [[arXiv:1412.6510](#)].
- [67] **IceCube** Collaboration, M. G. Aartsen et al., *An All-Sky Search for Three Flavors of Neutrinos from Gamma-Ray Bursts with the IceCube Neutrino Observatory*, *Astrophys. J.* **824** (2016), no. 2 115, [[arXiv:1601.06484](#)].
- [68] **IceCube** Collaboration, M. G. Aartsen et al., *Extending the search for muon neutrinos coincident with gamma-ray bursts in IceCube data*, *Astrophys. J.* **843** (2017), no. 2 112, [[arXiv:1702.06868](#)].
- [69] B. Zhou, M. Kamionkowski, and Y.-f. Liang, *Search for High-Energy Neutrino Emission from Radio-Bright AGN*, *Phys. Rev. D* **103** (2021), no. 12 123018, [[arXiv:2103.12813](#)].
- [70] N. Senno, K. Murase, and P. Mészáros, *Constraining high-energy neutrino emission from choked jets in stripped-envelope supernovae*, *JCAP* **01** (2018) 025, [[arXiv:1706.02175](#)].
- [71] A. Esmaili and K. Murase, *Constraining high-energy neutrinos from choked-jet supernovae with IceCube high-energy starting events*, *JCAP* **12** (2018) 008, [[arXiv:1809.09610](#)].
- [72] **IceCube** Collaboration, M. G. Aartsen et al., *IceCube Search for High-Energy Neutrino Emission from TeV Pulsar Wind Nebulae*, *Astrophys. J.* **898** (2020), no. 2 117, [[arXiv:2003.12071](#)].
- [73] S. Ando and K. Sato, *Relic neutrino background from cosmological supernovae*, *New J. Phys.* **6** (2004) 170, [[astro-ph/0410061](#)].
- [74] S. Horiuchi, J. F. Beacom, and E. Dwek, *The Diffuse Supernova Neutrino Background is detectable in Super-Kamiokande*, *Phys. Rev. D* **79** (2009) 083013, [[arXiv:0812.3157](#)].
- [75] **IceCube** Collaboration, C. Kopper, *Observation of Astrophysical Neutrinos in Six Years of IceCube Data*, *PoS ICRC2017* (2018) 981.
- [76] W. Hastings, *Monte Carlo Sampling Methods Using Markov Chains and Their Applications*, *Biometrika* **57** (1970) 97–109.
- [77] R. Barlow, *Asymmetric statistical errors*, in *Statistical Problems in Particle Physics, Astrophysics and Cosmology*, pp. 56–59, 6, 2004. [physics/0406120](#).